# A variable parameters auxiliary information based quality control chart with application in a spring manufacturing process: The Markov chain approach

Nger Ling Chong, Michael Khoo, Philippe Castagliola, Sajal Saha, Faijun Nahar Mim

# A variable parameters auxiliary information based quality control chart with application in a spring manufacturing process: the Markov chain approach

Nger Ling Chong
*School of Mathematical Sciences*
*Universiti Sains Malaysia, 11800 Minden, Penang, Malaysia*
*ngerlingc@gmail.com*

*Michael B. C. Khoo (Corresponding Author)
*School of Mathematical Sciences*
*Universiti Sains Malaysia, 11800 Minden, Penang, Malaysia*
*mkbc@usm.my*
Phone: 604-6533941
ORCID: 0000-0002-3245-1127

Philippe Castagliola
*Université de Nantes & LS2N UMR CNRS 6004, Nantes, France*
*philippe.castagliola@univ-nantes.fr*

Sajal Saha
*Department of Mathematics*
*International University of Business Agriculture and Technology*
*Bangladesh*
*sajal.saha@iubat.edu*

Faijun Nahar Mim
*School of Mathematical Sciences*
*Universiti Sains Malaysia, 11800 Minden, Penang, Malaysia*
faijun2005@yahoo.com

# A variable parameters auxiliary information based quality control chart with application in a spring manufacturing process: the Markov chain approach


## Abstract

In this paper, a new variable parameters chart for the process mean with a statistic that integrates information from the study and auxiliary variables is proposed. The proposed variable parameters chart with auxiliary information (AI) (abbreviated as VP-AI) is optimally designed to minimize the out-of-control steady-state (i) average time to signal ($ATS_1$) and (ii) expected average time to signal ($EATS_1$) values when the mean shift sizes are known and unknown, respectively. The Markov chain approach is adopted to derive the formulae of the performance measures $ATS_1$, standard deviation of the time to signal ($SDTS_1$) and $EATS_1$. The VP-AI chart significantly outperforms the standard VP chart; thus, justifying the incorporation of auxiliary information to enhance the ability of the VP chart. The VP-AI chart is also compared with the Shewhart AI, synthetic AI, exponentially weighted moving average (EWMA) AI, run sum AI and variable sample size and sampling interval (VSSI) AI charts. The VP-AI chart significantly outperforms the Shewhart AI, synthetic AI and VSSI AI charts for all levels of shifts. Meanwhile, the VP-AI chart outperforms the EWMA AI and run sum AI charts for most shifts. The VP-AI chart is found to be more robust than the EWMA-AI chart when the correlation coefficient is misspecified or the bivariate normality assumption is violated as long as the size of the shift is moderate or large. A real application which monitors spring elasticity is used to illustrate the VP-AI chart's implementation.



**Keywords:** control chart; variable parameters; auxiliary information; average time to signal; expected average time to signal

## 1. Introduction

To monitor and improve quality, the approach of using control charts in process monitoring has been widely adopted by researchers. Control charts which are extensively used in various manufacturing and service industries aid in enhancing the efficiency and quality of a process, thus reducing the amount of wastes produced and costs incurred. Recent studies on control charts can be found in Bourke (2020), Chong, Mukherjee, and Khoo (2020), Mehmood et al. (2019), Khatun et al. (2019), and Lawson (2019), to name a few. Due to the easy implementation of the basic Shewhart chart and its sensitivity in detecting large shifts in a process, the Shewhart chart has been widely adopted. However, the main drawback of the Shewhart chart is its lack of sensitivity in detecting small and moderate shifts. This is due to the fact that the Shewhart chart does not consider past process information. As a measure to improve the sensitivity of the Shewhart chart to small and moderate shifts, various control charting schemes have been proposed.

Traditionally, control charts use parameters, i.e. sample size, sampling interval, control and warning limits, that are fixed. However, using the same parameters lead to a lack of sensitivity to process shifts and an inefficient process monitoring (Yeong et al. 2018). Over the years, researchers have developed adaptive charts that take into account of past process information to overcome the setback of the basic Shewhart chart. An adaptive chart is a chart with one or more parameters that can vary in real time according to the location of the previous sample statistic plotted on the chart. The adaptive control scheme can be divided into four categories, which are the variable sample size (VSS), variable sampling interval (VSI), variable sample size and sampling interval (VSSI) and variable parameters (VP) charts. Some literature on adaptive charts can be found in Chong et al. (2019), Khoo et al. (2019), Castagliola et al. (2013), Hu et al. (2016), Yeong et al. (2018), Lee and Khoo (2018),

Reynolds et al. (1988), Tagaras (1998), Prabhu et al. (1994), Mahadik and Shirke (2009), Carot et al. (2002), Costa (1994), and Psarakis (2015).

For the VP chart, all the parameters of the chart are allowed to vary in real time. In other words, the selection of the sample size *n*, sampling interval *t*, and warning and control limits of the chart for the next inspection, depends on the location of the current sample statistic plotted on the chart. The VP chart is divided into three regions, namely the central, warning and out-of-control regions. When a sample point falls in the warning region, there is a higher tendency for the process to be out-of-control. Hence, control is tightened for the next inspection by taking a large sample size ($n_L$), short sampling interval ($t_S$), and tightened warning and control limits. In contrast, when the sample point falls in the central region, the tendency of the process to shift to an out-of-control condition is lower. Thus, we relax the control for the next inspection by taking a small sample size ($n_S$), long sampling interval ($t_L$), and loosened warning and control limits. The VP $\bar{X}$ chart that monitors the mean of a process was developed by Costa (1999). Meanwhile, Yeong et al. (2018) proposed a VP chart that monitors the coefficient of variation (CV) and found that the VP CV chart consistently surpasses the other five competing CV charts in the literature. For other research works on the VP chart, readers can refer to Chen and Chang (2008), Lin and Chou (2007), Guo, Cheng, and Lu (2014) and Wang et al. (2018).

To improve the process monitoring of the quality characteristic of interest, cause-selecting and regression-adjusted control charts (see Mandel (1969), Zhang (1985), Wade and Woodall (1993), Shu, Tsung and Tsui (2005), to name a few) utilize the correlation between the quality characteristic of interest and the associated quality characteristic(s). In fact, the construction of the cause-selecting and regression-adjusted control charts involve the adjustment of the effect of the associated quality characteristic(s) to monitor the quality characteristic of interest (i.e. obtaining residuals to monitor the quality characteristic of

interest) (Riaz 2008). Similarly, by utilising the relationship between the auxiliary variable and quality characteristic of interest in auxiliary information (AI) charts, the accuracy in which parameters are estimated can be enhanced. It is a common practice to apply the AI concept in survey sampling to obtain more accurate estimates of the population parameters. For an improved estimator precision, the auxiliary or also known as supplementary information can be utilised in both design and estimation stages (Haq and Khoo 2016). In order to improve process monitoring, researchers have integrated the concept of auxiliary information with control charting schemes. With a regression estimator that incorporates information from an auxiliary or supplementary variable, the precision of an estimator can be enhanced which leads to a more sensitive control chart. The auxiliary variable concept can be used in various fields. For example, in a platinum refinery, when the quantity of platinum metal is the study variable or quality characteristic, the auxiliary variable considered can be the quantity of other metals which are generally correlated to the quantity of platinum metal (Ahmad et al. 2014). Additionally, when monitoring the process of generating power from coal, the study variable monitored can be the total power generated, while the auxiliary variable used can be the air temperature or quantity of flue gas (Ahmad et al. 2014). In a fibre production process, the auxiliary information from the weight of textile fibres can be used to improve the monitoring of the study variable which is the single-strand break factor (Haq and Khoo 2016).

Riaz (2008) proposed a Shewhart chart with auxiliary information (SH-AI) that improves the monitoring of process mean. Furthermore, Abbas, Riaz, and Does (2014) proposed an exponentially weighted moving average (EWMA) control chart with auxiliary information (EWMA-AI) and found that their proposed chart is effective in detecting small and moderate shifts. Haq and Khoo (2016) proposed a synthetic control chart with auxiliary information (SYN-AI). Meanwhile, Ng et al. (2018) proposed the run sum chart with

auxiliary information (RS-AI) and showed that the RS-AI chart outperforms the SH-AI, SYN-AI and EWMA-AI charts for all shifts given that the correlation $\rho$ is large. Saha et al. (2018) developed the VSSI chart with auxiliary information (VSSI-AI) which surpasses the EWMA-AI and SYN-AI charts. Research works on control charts with auxiliary information can also be found in Ahmad et al. (2014), Riaz (2011), Abbasi and Riaz (2016), Riaz et al. (2013) and Lee et al. (2015), to name a few.

Motivated by the improved effectiveness of control charts through the incorporation of auxiliary information in the literature, a new VP chart that utilises auxiliary information (VP-AI) is developed in this paper by integrating two powerful control charting approaches which are the variable parameters method and auxiliary information technique. In control charting literature, it is a common practice to integrate effective control charting procedures to construct a new and superior control chart to improve process monitoring. To the best of the authors' knowledge, the VP-AI chart is not present in the literature and this paper is presented to fill the gap. In this paper, the VP-AI chart is studied and compared with its standard VP counterpart and existing SH-AI, SYN-AI, EWMA-AI, RS-AI and VSSI-AI charts, in terms of the steady-state average time to signal (ATS), standard deviation of the time to signal (SDTS) and expected ATS (EATS) criteria. Note that the VP-AI chart is equivalent to the standard VP chart when the correlation coefficient $\rho = 0$. The proposed VP-AI chart outperforms the SH-AI, SYN-AI and VSSI-AI charts for all shifts while surpassing the EWMA-AI and RS-AI charts for most shifts. Additionally, the VP-AI chart surpasses its standard VP counterpart. This paper also contributes to the AI control charting literature by studying the robustness of the VP-AI chart. Traditionally, when designing an AI chart, it is assumed that (i) $\rho$ is not misspecified and (ii) the study variable $X$ and auxiliary variable $M$ follow the bivariate normal distribution. In this paper, the robustness of the VP-AI chart when violations in (i) or (ii) occurs is studied and compared with the EWMA-AI chart.

The rest of this paper is organized as follows: Section 2 discusses the concept of auxiliary information. In Section 3, the overview, performance measures and optimization algorithm of the VP-AI chart are outlined and discussed. A numerical analysis of the VP-AI chart is given in Section 4 while the VP-AI chart is compared with the five existing AI charts in Section 5. In Section 6, the robustness of the VP-AI chart is evaluated and compared with the EWMA-AI chart for the case where $\rho$ is misspecified or the bivariate normality assumption is violated. To illustrate the implementation of the VP-AI chart, an illustrative example is provided in Section 7 using the dataset from a spring manufacturing process. Lastly, Section 8 completes the paper with conclusions and suggestions for future research.

## 2. Properties of the auxiliary information approach

In practice, it may be time-consuming and costly to measure a quality characteristic of interest which we refer to as the study variable *X*. Hence, obtaining an efficient estimation of the population mean $\mu_X$ of *X*, with a desired accuracy, is sometimes impossible. Thus, another characteristic that is correlated with the quality characteristic of interest, known as the auxiliary variable *M* can be measured. By employing information from both study and auxiliary variables, an estimation of $\mu_X$ with an enhanced accuracy can be obtained. The VP-AI chart is a univariate chart as it monitors only the mean shifts in *X* but it is designed based on a regression estimator that incorporates information obtained from both *X* and *M*. In other words, the design of the VP-AI chart is based on a test statistic that requires information from both the study variable and auxiliary variable but only detects shifts related to the process mean of the study variable *X* (one variable only). Along with the study variable, data on several related auxiliary variables are often available, but only one auxiliary variable which is correlated to the study variable is considered in this paper.

Suppose that $X$ and $M$ are correlated, and $(X,M)$ follows a bivariate normal distribution such that $(X,M) \sim N_2(\mu_X, \mu_M, \sigma_X^2, \sigma_M^2, \rho)$. The population mean and variance of $X$ are denoted by $\mu_X = \mu_{X0} + \delta\sigma_X$ and $\sigma_X^2$, respectively, where $\delta = \frac{|\mu_X - \mu_{X0}|}{\sigma_X}$ represents the size of the standardized mean shift of *X*. Meanwhile, the population mean and variance of *M* are denoted by $\mu_M$ and $\sigma_M^2$, respectively, and the correlation coefficient between the variables *X* and *M* is denoted by $\rho$.

Let $(X_j, M_j)$, where $j = 1,2,...,n(r)$ be a bivariate random sample from a bivariate normal distribution such that the sample size of a random sample *r* is $n(r)$. The regression estimator of $\mu_X$ is as follows (Riaz 2008):

$$Y_{X_r}^* = \bar{X}_r + \beta(\mu_M - \bar{M}_r), \tag{1}$$

such that $\beta = \rho\left(\frac{\sigma_X}{\sigma_M}\right)$. For the *r*th sample, the sample mean of *X* is $\bar{X}_r = \frac{1}{n(r)}\sum_{j=1}^{n(r)} X_j$, while the sample mean of *M* is $\bar{M}_r = \frac{1}{n(r)}\sum_{j=1}^{n(r)} M_j$. Note that $Y_{X_r}^*$ has mean and variance (Riaz 2008)

$$E(Y_{X_r}^*) = \mu_X \tag{2}$$

and

$$Var(Y_{X_r}^*) = \frac{1}{n(r)}\sigma_X^2(1-\rho^2), \tag{3}$$

respectively, such that $Y_{X_r}^* \sim N(\mu_X, (1/n(r))\sigma_X^2(1-\rho^2))$.

**3. Variable parameters control chart with auxiliary information**

Section 3 consists of three subsections. Section 3.1 provides an overview of the VP-AI chart. Subsequently, the formulae of the steady state ATS, SDTS and EATS are outlined in Section 3.2. Lastly, the optimization algorithms of the VP-AI chart that minimize the out-of-control ATS and EATS, denoted by $ATS_1$ and $EATS_1$, respectively, are given in Section 3.3.

### 3.1 Overview of the VP-AI chart

Assume that $Y_{X_r}^*$, for $r = 1, 2, \ldots$, from Equation (1) is the quality characteristic to be monitored. The charting statistic plotted on the VP-AI chart is

$$Z_r = \frac{\sqrt{n(r)}\left(Y_{X_r}^* - \mu_{X0}\right)}{\sigma_X \sqrt{1-\rho^2}} \quad . \tag{4}$$

When the process is in-control $(\delta = 0)$, $E\left(Y_{X_r}^*\right) = \mu_{X0}$ and $Z_r$ follows the standard normal distribution, i.e. $Z_r \sim N(0,1)$.

For a standard SH-AI chart with fixed parameters, practitioners take a sample with size $n_0$ at every sampling interval $t_0$ with a fixed control limit $K_0$. However, the SH-AI chart is only effective in detecting large shifts. The VP-AI chart enhances the performance of the SH-AI chart toward small and moderate shifts by considering past process information. Similar to the VP chart, the VP-AI chart consists of three regions (i.e. central, warning and out-of-control) that are divided by the warning ($\pm W$) and control ($\pm K$) limits. Note that the upper and lower warning limits are denoted by $W$ and $-W$, respectively, while the upper and lower control limits are denoted by $K$ and $-K$, respectively. The region $[-W, W]$ is the central region, while the regions $(W, K]$ and $(-K, -W]$ are the warning regions. The chart's parameters vary according to the most recent process information. In other words, depending on the location of the sample statistic plotted on the VP-AI chart, each parameter of the chart (sample size, sampling interval, control and warning limits) can alternate between two values.

The schematic representation that shows the operation of the VP-AI chart is given in Figure 1.

-- Insert Figure 1 here --

The VP-AI chart works as follows:

- When $Z_r$ lies in the central region $(Z_r \in I_1)$, there is a lower tendency for the process to shift to an out-of-control condition. Hence, the next sample size is small $n_S$ $(< n_0 < n_L)$ and taken after a long sampling interval $t_L$ $(> t_0 > t_S)$. Additionally, $Z_{r+1}$ is plotted on the VP-AI chart using loosened control and warning limits to relax the control, i.e. $K_1 (> K_0 > K_2)$, $-K_1 (< -K_0 < -K_2)$, $W_1 (> W_2)$ and $-W_1 (< -W_2)$.
- When $Z_r$ lies in the warning region $(Z_r \in I_2)$, there is a higher tendency for the process to shift to an out-of-control condition. Thus, the next sample size is large $n_L$ $(> n_0 > n_S)$ and taken after a short sampling interval $t_S$ $(< t_0 < t_L)$. Furthermore, $Z_{r+1}$ is plotted on the VP-AI chart using tightened control and warning limits to tighten the control, i.e. $K_2 (< K_0 < K_1)$, $-K_2 (> -K_0 > -K_1)$, $W_2 (< W_1)$ and $-W_2 (> -W_1)$.
- Lastly, if $Z_r$ lies in the out-of-control region $(Z_r \in I_3)$, a signal is issued by the VP-AI chart to indicate an out-of-control condition and corrective actions have to be swiftly taken to remove the assignable cause(s).

It is worth noting that Figure 1 consists of two scales. If $Z_r$ lies in the central region, the loosened scale on the *left* is used to plot $Z_{r+1}$ on the VP-AI chart. On the other hand, if $Z_r$ lies in the warning region, the tightened scale on the *right* is used to plot $Z_{r+1}$ on the VP-AI chart.

### 3.2 Performance measures

The average run length (ARL) is extensively adopted to study the performance of a control chart. However, it is not a suitable performance measure for the VP-AI chart as the sampling interval is allowed to vary. Hence, in this paper, we adopt the steady state ATS which is defined as the expected time from the process mean shift until an out-of-control condition is signaled by the chart to evaluate the performance of the VP-AI chart. It is assumed that the process is in-control initially and the process mean shift occurs at some time in the future.

In this paper, the Markov chain approach is adopted for the computation of the ATS. The Markov chain consists of three states where the first state corresponds to the central region, the second state corresponds to the warning region and the third state corresponds to the out-of-control region (Yeong et al. 2018). The first and second states are transient while the third state is absorbing. Hence, the transition probability matrix (tpm) **P** is

$$\mathbf{P}=\begin{pmatrix}\mathbf{Q} & (\mathbf{I}-\mathbf{Q})\mathbf{1}\\ \mathbf{0}^T & 1\end{pmatrix}=\begin{pmatrix}P_{11} & P_{12} & 1-P_{11}-P_{12}\\ P_{21} & P_{22} & 1-P_{21}-P_{22}\\ 0 & 0 & 1\end{pmatrix} \tag{5}$$

such that **Q** represents a 2×2 tpm for the transient states, **I** represents a 2×2 identity matrix, **1** is a 2×1 column vector with all elements equal to unity and $\mathbf{0}^T=(0,0)$. The transition probabilities in **Q** are $P_{11}, P_{12}, P_{21}$ and $P_{22}$ which are given as

$$\begin{aligned}P_{11}&=\Pr\left(-W_1<Z_r<W_1\mid n_S,\delta\right)\\&=\Phi\left(W_1-\delta\sqrt{\frac{n_S}{1-\rho^2}}\right)-\Phi\left(-W_1-\delta\sqrt{\frac{n_S}{1-\rho^2}}\right),\end{aligned} \tag{6}$$

$$\begin{aligned}P_{12}&=\Pr\left(-K_1<Z_r<-W_1\mid n_S,\delta\right)+\Pr\left(W_1<Z_r<K_1\mid n_S,\delta\right)\\&=\Phi\left(-W_1-\delta\sqrt{\frac{n_S}{1-\rho^2}}\right)-\Phi\left(-K_1-\delta\sqrt{\frac{n_S}{1-\rho^2}}\right)+\\&\quad\Phi\left(K_1-\delta\sqrt{\frac{n_S}{1-\rho^2}}\right)-\Phi\left(W_1-\delta\sqrt{\frac{n_S}{1-\rho^2}}\right),\end{aligned} \tag{7}$$

$$P_{21} = \Pr\left(-W_2 < Z_r < W_2 \mid n_L, \delta\right) = \Phi\left(W_2 - \delta\sqrt{\frac{n_L}{1-\rho^2}}\right) - \Phi\left(-W_2 - \delta\sqrt{\frac{n_L}{1-\rho^2}}\right), \tag{8}$$

$$P_{22} = \Pr\left(-K_2 < Z_r < -W_2 \mid n_L, \delta\right) + \Pr\left(W_2 < Z_r < K_2 \mid n_L, \delta\right) = \Phi\left(-W_2 - \delta\sqrt{\frac{n_L}{1-\rho^2}}\right) - \Phi\left(-K_2 - \delta\sqrt{\frac{n_L}{1-\rho^2}}\right) + \Phi\left(K_2 - \delta\sqrt{\frac{n_L}{1-\rho^2}}\right) - \Phi\left(W_2 - \delta\sqrt{\frac{n_L}{1-\rho^2}}\right), \tag{9}$$

where $\Phi(.)$ is the standard normal distribution function. The VP-AI chart is equivalent to the standard VP chart when $\rho = 0$. The steady-state ATS is computed as

$$\mathrm{ATS} = \mathbf{b}^T(\mathbf{I} - \mathbf{Q})^{-1}\mathbf{t}, \tag{10}$$

where $\mathbf{t}^T = (t_L, t_S)$ is the vector of sampling intervals and $\mathbf{b}^T = (b_1, b_2)$ represents the steady-state probability vector such that $b_1 + b_2 = 1$. Note that $b_1$ and $b_2$ represent the probabilities of being in the central and warning regions, respectively such that

$$b_1 = \frac{P_{11}^0}{P_{11}^0 + P_{12}^0} \tag{11a}$$

and

$$b_2 = \frac{P_{22}^0}{P_{21}^0 + P_{22}^0}, \tag{11b}$$

where $P_{11}^0, P_{12}^0, P_{21}^0$ and $P_{22}^0$ are computed with Equations (6) - (9), respectively by setting $\delta = 0$. $\mathrm{ATS}_1$ is the ATS corresponding to the out-of-control case ($\delta > 0$) while $\mathrm{ATS}_0$ corresponds to the in-control case ($\delta = 0$). A chart with lower $\mathrm{ATS}_1$ values is more effective in detecting process mean shifts. Thus, when the $\mathrm{ATS}_0$ is fixed, a chart which has smaller $\mathrm{ATS}_1$ in comparison to other charts is superior. Meanwhile, the out-of-control SDTS ($\mathrm{SDTS}_1$) is also considered as a performance measure to gain insight about the spread of the time to signal distribution. The SDTS can be computed as follows (Yeong et al. 2018):

$$\text{SDTS} = \sqrt{a}\,, \tag{12}$$

where $a = \mathbf{b}^T(\mathbf{I}-\mathbf{Q})^{-1}\left(2\mathbf{D}_\mathbf{t}(\mathbf{I}-\mathbf{Q})^{-1}\mathbf{t}-\mathbf{t}^{(2)}\right)-\text{ATS}^2$. Note that $\mathbf{D}_\mathbf{t}$ is the diagonal matrix with diagonal elements from $\mathbf{t}$ while $\mathbf{t}^{(2)}$ represents the squares of vector $\mathbf{t}$ elements.

The computation of ATS requires the specification of the shift size $\delta$ in advance. However, in practice, the value of $\delta$ is unknown prior to the occurrence of the shift. Hence, the EATS that is computed based on a shift interval $(\delta_{\min},\delta_{\max})$ is adopted as an alternative to ATS and the computation of EATS is as follows:

$$\text{EATS} = \int_{\delta_{\min}}^{\delta_{\max}} \text{ATS}(\delta)\, f(\delta)\, d\delta \tag{13}$$

such that $\delta_{\min}$ and $\delta_{\max}$ denote the minimum and maximum process mean shifts for the interval $(\delta_{\min},\delta_{\max})$, respectively. Additionally, $\text{ATS}(\delta)$ is computed based on Equation (10) and $f(\delta)$ represents the probability density function (pdf) of the shift $\delta$. By assuming that there is an equal probability of occurrence of $\delta$ in $(\delta_{\min},\delta_{\max})$, then the distribution of $\delta$ is uniform, i.e. $\delta \sim U(\delta_{\min},\delta_{\max})$ (Sparks 2000). Hence, as a result of the uniform distribution, Equation (13) becomes

$$\text{EATS} = \frac{1}{\delta_{\max}-\delta_{\min}} \int_{\delta_{\min}}^{\delta_{\max}} \text{ATS}(\delta)\, d\delta\,, \tag{14}$$

which is approximated with the Gauss-Legendre quadrature as the integral cannot be evaluated exactly. $\text{EATS}_1$ is the EATS corresponding to the out-of-control case ($\delta > 0$) while $\text{EATS}_0 = \text{ATS}_0$ corresponds to the in-control case ($\delta = 0$).

### 3.3 Optimization algorithm

This section explains the algorithms used to compute the optimal parameters $n_S, n_L, t_S, t_L, K_1, K_2, W_1$ and $W_2$ of the VP-AI chart. The optimization program of the VP-AI

chart is written in the ScicosLab software and the results are verified with simulation in the Statistical Analysis System (SAS) software. In this paper, there are two optimization criteria considered. The first optimization criterion involves the minimization of $\mathrm{ATS}_1$ when $\delta$ is known in advance while the second optimization criterion involves the minimization of $\mathrm{EATS}_1$ when $\delta$ is unknown in advance. The first optimization criterion can be formulated by the model shown below:

$$\text{Objective function: Minimize } \mathrm{ATS}_1 \tag{15}$$

subject to three constraints that ensure a fair comparison, given by (Costa 1999)

$$b_1 n_S + b_2 n_L = n_0, \tag{16}$$

$$b_1 t_L + b_2 t_S = t_0 \tag{17}$$

and

$$b_1 \Pr\left(|Z_r| > K_1\right) + b_2 \Pr\left(|Z_r| > K_2\right) = \Pr\left(|Z_r| > K_0\right), \tag{18}$$

such that $n_0$, $t_0$ and $K_0$ are the fixed parameters of the SH-AI chart and $\Pr\left(|Z_r| > K_0\right) = 1/\mathrm{ATS}_0$ . The in-control performance of the VP-AI chart has to be equal with the competing charts for a fair comparison among the charts. Thus, the constraints in Equations (16) - (18) set the in-control average sample size ($\mathrm{ASS}_0$) as $n_0$, in-control average sampling interval ($\mathrm{ASI}_0$) as $t_0$ and ensure that the false alarm rates are the same, respectively. Using the constraints in Equations (11a) and (16), the values of $W_i$ such that $i = 1, 2$ can be computed with (Costa 1999)

$$W_i = \Phi^{-1}\left[\frac{2(n_L - n_0)\Phi(K_i) + n_0 - n_S}{2(n_L - n_S)}\right], \tag{19}$$

while it follows from Equation (18) that

$$t_L = \frac{t_0(n_L - n_S) - t_S(n_0 - n_S)}{n_L - n_0}. \tag{20}$$

In this paper, $K_1 = 6$, $t_0 = 1$ and $\text{ATS}_0 = 370$ are employed. These are the steps employed to compute the optimal parameters of the VP-AI chart by minimizing $\text{ATS}_1(\delta)$ for a specific $\delta$.

1. Specify the values of $\delta, \rho, t_0, t_S, n_0, K_1$ and $\text{ATS}_0$ while initializing $\text{ATS}_{\min} = \infty$. The value of $t_S$ is specified to avoid the possibility of obtaining an extremely small value as very frequent sampling is not practical in a real-life scenario (Yeong et al. 2018).
2. Initialize $n_S = 2$.
3. Initialize $n_L = n_0 + 1$.
4. Determine the value of $K_2$ such that the specified $\text{ATS}_0$ value in Step 1 is acquired.
5. Meanwhile, the values of $W_1$ and $W_2$ are computed using Equation (19).
6. Using Equation (20), compute the value of $t_L$.
7. With the values of the parameters $n_S, n_L, t_S, t_L, K_1, K_2, W_1$ and $W_2$ obtained prior to this step, compute the value of $\text{ATS}_1$ using Equation (10).
8. If $\text{ATS}_1 < \text{ATS}_{\min}$, let $\text{ATS}_{\min} = \text{ATS}_1$.
9. With the same value of $n_S$, increase $n_L$ by 1.
10. If $n_L \leq 31$, repeat Steps 4 to 9.
11. Increase the value of $n_S$ by 1.
12. If $n_S \leq n_0 - 1$, repeat Steps 4 to 11.

Based on the outputs computed using the steps above, the parameters $n_S, n_L, t_S, t_L, K_1, K_2, W_1$ and $W_2$ that result in the lowest $\text{ATS}_1$ value are the optimal parameters. The $\text{SDTS}_1$ values are then computed based on these optimal parameters. The second optimization criterion can be formulated by the model shown below:

$$\text{Objective function: Minimize } \text{EATS}_1 \tag{21}$$

subject to the constraints in Equations (16) - (18). Steps (1) to (12) can also be employed for the second optimization criterion by substituting $\delta$ with $\left(\delta_{\min}, \delta_{\max}\right)$ and computing $\text{EATS}_1$ using Equation (14) instead of $\text{ATS}_1$. Note that $\text{EATS}_0$ is equal to the $\text{ATS}_0$ value specified in Step (1).

## 4. Numerical analysis

In this section, the performance of the VP-AI chart is evaluated. This section presents the optimal parameters $n_S, n_L, t_S, t_L, K_1, K_2, W_1$ and $W_2$ that (i) minimize $\text{ATS}_1$ and (ii) minimize $\text{EATS}_1$ subject to the constraints $\text{ASS}_0 = n_0$, $\text{ASI}_0 = t_0$ and $\text{ATS}_0 = 370$. For (i), $t_S \in \{0.01, 0.1\}$, $n_0 \in \{5, 7\}$, $\rho \in \{0, 0.25, 0.5, 0.75, 0.9, 0.95\}$ and $\delta \in \{0.2, 0.4, 0.6, 0.8, 1, 1.5, 2\}$ are considered in this paper and the optimal parameters with their corresponding $\text{ATS}_1$ and $\text{SDTS}_1$ are shown in Tables 1 and 2. Meanwhile, for (ii), we consider $t_S \in \{0.01, 0.1\}$, $n_0 \in \{5, 7\}$, $\rho \in \{0, 0.25, 0.5, 0.75, 0.9, 0.95\}$ and $(\delta_{\min}, \delta_{\max}) \in \{(0.2, 0.6), (0.5, 1), (1, 1.5), (1.5, 2)\}$ and the optimal parameters with their corresponding $\text{EATS}_1$ are shown in Tables 3 and 4.

When the process is out-of-control, lower $\text{ATS}_1$ values indicate a better performance of the chart as less time is required to detect an out-of-control condition. In other words, the chart has a better ability in detecting mean shifts when the $\text{ATS}_1$ values are lower for an out-of-control process. From Tables 1 and 2, it can be seen that the $\text{ATS}_1$ values decrease as $\delta$ increases which implies that the VP-AI chart requires less time to detect larger mean shifts. This is justified by the need to quickly detect larger shifts that result in a significant loss of quality. As the $\text{ATS}_1$ values become smaller when $\rho$ increases across all values of $n_0$, it can be deduced that the VP-AI chart surpasses the standard VP chart ($\rho = 0$), thus justifying the integration of auxiliary information. To illustrate, when $\delta = 0.2$ and $n_0 = 5$ in Table 1, $\text{ATS}_1$ = 55.28 (for $\rho = 0$) decreases to $\text{ATS}_1$ = 3.11 (for $\rho = 0.95$). Additionally, the outperformance

of the VP-AI chart in comparison to the standard VP chart increases with $\rho$. This implies that the sensitivity of the VP-AI chart is enhanced with an increase in $\rho$. Hence, utilising information from the auxiliary variable has enhanced the ability of the VP chart in detecting process mean shifts. Furthermore, an increase in the sample size $n_0$ results in a decrease in the $ATS_1$ values for all shifts. Thus, a larger sample size enhances the sensitivity of the VP-AI chart as an out-of-control condition is signalled earlier. For example, consider Table 1 when $\rho = 0.25$ and $\delta$ = 0.2, the $ATS_1$ = 51.37 (for $n_0 = 5$) decreases to $ATS_1$ = 39.98 (for $n_0 = 7$). By comparing Tables 1 and 2, there is only a slight difference in the performance of the VP-AI chart when $t_S = 0.01$ in comparison to $t_S = 0.1$. The $SDTS_1$ values of the standard VP chart ($\rho$ = 0) are higher than that of the VP-AI chart for all shifts, indicating that the former has a larger spread of the time to signal distribution; thus, the latter is superior to the former.

-- Insert Table 1 here--

-- Insert Table 2 here--

To obtain the results in Tables 1 and 2, it is assumed that the value of $\delta$ can be specified in advance. However, in practice, $\delta$ values cannot be specified a priori. Alternatively, $EATS_1$ is computed based on a range of shifts $(\delta_{\min}, \delta_{\max})$ to account for the case when we cannot specify the exact shift size in advance. The optimal parameters and their corresponding $EATS_1$ values are shown in Tables 3 and 4. For all values of $n_0$, the $EATS_1$ values when $\rho > 0$ are lower than the corresponding $EATS_1$ values when $\rho = 0$, which implies that the VP-AI chart surpasses the standard VP chart. Additionally, the $EATS_1$ values decrease when $\rho$ increases. As can be seen in Table 3, the $EATS_1$ values for the range of shifts $(\delta_{\min}, \delta_{\max})$ that covers larger $\delta$ values are lower, thus the VP-AI chart requires less time to detect the range of shifts $(\delta_{\min}, \delta_{\max})$ covering larger values of $\delta$. As an illustration,

when $\rho = 0.5$ and $n_0 = 5$ in Table 3, $\text{EATS}_1 = 11.04$ when $(\delta_{\min}, \delta_{\max}) = (0.2, 0.6)$ reduces to $\text{EATS}_1 = 1.00$ when $(\delta_{\min}, \delta_{\max}) = (1.5, 2)$. Similar to the case with known shift sizes, by increasing the value of $n_0$, the performance of the VP-AI chart improves. Furthermore, there is only a minimal effect on $\text{EATS}_1$ when $t_S$ is varied (see Tables 3 and 4).

-- Insert Table 3 here --

-- Insert Table 4 here --

## 5. Comparative studies

In this paper, the performance of the VP-AI chart is compared with five competing charts, in terms of the $\text{ATS}_1$, $\text{SDTS}_1$ and $\text{EATS}_1$ criteria. The first and second criteria are used to compare the charts when the exact shift size, $\delta$ is known and unknown in advance, respectively. The chart that has lower $\text{ATS}_1$ and $\text{EATS}_1$ values has a superior performance as a shorter amount of time to detect an out-of-control condition is required. Meanwhile, the chart with lower $\text{SDTS}_1$ values is more effective as the spread of the time to signal distribution is smaller. Specifically, in this paper, the competing charts that are compared with the VP-AI chart are the SH-AI, SYN-AI, EWMA-AI, RS-AI and VSSI-AI charts. In this paper, to ensure a fair comparison can be made among the charts, the constraints $\text{ASS}_0 = n_0$, $\text{ASI}_0 = 1$ and $\text{ATS}_0 = 370$ have to be adhered to. Note that for the SH-AI, SYN-AI, EWMA-AI and RS-AI charts that have a fixed sampling interval, $t_0$ is set as 1 to ensure that $\text{ATS}_1 = \text{ARL}_1$.

For more information on the designs of the SH-AI, SYN-AI, EWMA-AI, RS-AI and VSSI-AI charts, readers can refer to Riaz (2008), Haq and Khoo (2016), Abbas et al. (2014), Ng et al. (2018) and Saha et al. (2018), respectively. The VP-AI and VSSI-AI charts are adaptive charts with parameters that can be varied depending on the location of the sample

statistic plotted on the chart. For the VSSI-AI chart, two parameters (sample size and sampling interval) are varied, while the VP-AI chart varies all parameters (sample size, sampling interval, and control and warning limits). By comparing the performance of the VP-AI and VSSI-AI charts, the effect of varying the control and warning limits can be studied. The VP-AI chart is also compared with the RS-AI chart. Although the RS-AI chart proposed by Ng et al. (2018) consists of 4 and 7 regions, only the RS-AI chart with 7 regions that has a superior performance compared to its 4 regions counterpart is considered in this paper. Similar to the RS-AI chart, the VP-AI chart is also compared with the SH-AI, SYN-AI and EWMA-AI charts. It is worth noting that the run length properties of the EWMA-AI chart considered in this paper is derived with the Markov chain approach and not computed through simulation as in Abbas et al. (2014). As a result of space constraints and the minimal effect of varying $t_S$ as shown in Section 4, we only consider $t_S = 0.01$ in this section. Tables 5 and 6 show the comparison among the charts, in terms of the $\text{ATS}_1$ and $\text{SDTS}_1$ criteria, respectively, where the exact shift size, $\delta$ is assumed to be known a priori for $t_S = 0.01$, $\text{ATS}_0 = 370$, $n_0 \in \{5,7\}$, $\rho \in \{0, 0.25, 0.5, 0.75, 0.9, 0.95\}$ and $\delta \in \{0.2, 0.4, 0.6, 0.8, 1, 1.5, 2\}$.

-- Insert Table 5 here –

Based on Table 5, the VP-AI chart significantly outperforms the SH-AI, SYN-AI and VSSI-AI charts for all shift sizes across all $\rho$ and $n_0$ values. To illustrate, when $n_0 = 5, \delta = 0.2$ and $\rho = 0.25$, the VP-AI chart is 3.3 (171.05 / 51.37), 2.8 (142.28 / 51.37) and 2.5 (127.08 / 51.37) times faster than the SH-AI, SYN-AI and VSSI-AI charts, respectively in detecting mean shifts (see Table 5). The outperformance of the VP-AI chart in comparison to the VSSI-AI chart implies that the monitoring of process mean is enhanced by varying the control and warning limits. Even though the VP-AI chart is more complex than the VSSI-AI chart, as the VP-AI chart involves the additional step of varying the control and warning limits, the complexity is justified as the VP-AI chart is more effective and significantly

outperforms the VSSI-AI chart for all shift sizes across all $\rho$ and $n_0$ values. The computation time to solve the required optimization for the VP-AI chart due to the additional complexity only differs slightly from the VSSI-AI chart. By comparing the VP-AI and EWMA-AI charts, it can be seen that, for all values of $n_0$, the VP-AI chart is superior to the EWMA-AI chart for all shifts when $\rho \geq 0.9$ while the VP-AI chart surpasses the EWMA-AI chart for all shifts except $\delta = 0.2$ when $\rho \leq 0.75$. As an example, the VP-AI is 1.8 $(5.46/3.11)$ times faster than the EWMA-AI chart in detecting mean shifts when $n_0 = 5,\ \delta = 0.2$ and $\rho = 0.95$, while the VP-AI chart is 1.2 $(10.59/9.02)$ times faster than the EWMA-AI chart in shift detection when $n_0 = 5,\ \delta = 0.4$ and $\rho = 0.25$ (see Table 5). In short, the VP-AI chart outperforms the EWMA-AI chart for detecting all shift sizes when $\rho$ = 0.95. A comparison of the VP-AI chart with the RS-AI chart shows that the VP-AI chart is superior to the RS-AI chart for all shifts when $n_0 = 5$. Meanwhile, for $n_0 = 7$, the VP-AI chart outperforms the RS-AI chart for all shifts when $\rho \geq 0.75$ while the VP-AI chart outperforms the RS-AI chart for all shifts except $\delta = 0.2$ when $\rho \leq 0.5$. Hence, the VP-AI chart outperforms the RS-AI chart for most shifts.

-- Insert Table 6 here –

In Table 6, it can be seen that the $SDTS_1$ values of the VP-AI chart are generally lower than that of the SH-AI, SYN-AI and VSSI-AI charts, especially when the shift size, $\delta <$ 0.8. This implies that the VP-AI chart has a smaller spread of the time to signal distribution in comparison with the SH-AI, SYN-AI and VSSI-AI charts for small and moderate shifts. To illustrate, when $\delta$ = 0.2, $\rho$ = 0.25 and $n_0$ = 5, the spread of the time to signal distribution for the SH-AI, SYN-AI and VSSI-AI charts are 3.30 (170.71/ 51.72), 2.71 (140.33 / 51.72) and 2.46 (127.25 / 51.72) times larger than that of the VP-AI chart (see Table 6). A comparison of the $SDTS_1$ values of the VP-AI and RS-AI charts when $n_0$ = 5 shows that the VP-AI chart is

superior to the RS-AI chart when $\delta \leq 0.6$ for $\rho \leq 0.75$, and $\delta = 0.2$ for $\rho = 0.9$ and 0.95 (see Table 6). When comparing the VP-AI and RS-AI charts for $n_0 = 7$, the RS-AI chart has smaller $SDTS_1$ values for most shift sizes $\delta$ but when $\delta$ increases the difference in the $SDTS_1$ values between the two charts generally decreases. The EWMA-AI chart has a smaller spread of the time to signal distribution in comparison with the VP-AI chart but the difference in $SDTS_1$ values generally decreases with $\delta$.

As mentioned in Section 4, in practice, the exact shift size is usually unknown a priori. Hence, the performance measure $EATS_1$ is adopted and compared with the corresponding $EATS_1$ of the SH-AI, SYN-AI, EWMA-AI, RS-AI and VSSI-AI charts when $t_S = 0.01$, $EATS_0 = 370$, $n_0 \in \{5,7\}$, $\rho \in \{0, 0.25, 0.5, 0.75, 0.9, 0.95\}$ and $(\delta_{\min}, \delta_{\max}) \in \{(0.2, 0.6), (0.5, 1), (1, 1.5), (1.5, 2)\}$ as shown in Table 7. When the exact shift size, $\delta$ cannot be specified in advance, the VP-AI chart outperforms the SH-AI, SYN-AI and RS-AI charts for all ranges of shifts $(\delta_{\min}, \delta_{\max})$ considered, irrespective of the values of $\rho$ and $n_0$. Meanwhile, the VP-AI chart outperforms the VSSI-AI chart for most ($\delta_{\min}$, $\delta_{\max}$), $\rho$ and $n_0$ values (with the exception of $n_0 = 7$, $\rho = 0$ and ($\delta_{\min}$, $\delta_{\max}$) = (1, 1.5), where the VSSI-AI chart performs slightly better) (see Table 7). On the other hand, when $n_0 = 5$, the VP-AI chart is superior to the EWMA-AI chart for all shift sizes when $\rho \geq 0.75$ while the VP-AI chart surpasses the EWMA-AI chart for all shift sizes, except ($\delta_{\min}$, $\delta_{\max}$) = (0.2, 0.6) when $\rho \leq 0.5$. Meanwhile, when $n_0 = 7$, the VP-AI chart surpasses the EWMA-AI chart for all shift sizes (with the exception of $\rho = 0$ and ($\delta_{\min}$, $\delta_{\max}$) = (0.2, 0.6)). Thus, the VP-AI chart outperforms the EWMA-AI chart for most ranges of shifts $(\delta_{\min}, \delta_{\max})$ when the exact shift size cannot be specified.

-- Insert Table 7 here --

## 6. Robustness of the VP-AI chart under misspecifications of $\rho$ and violation of bivariate normality

The analyses in the preceding sections assume that the values of $\rho$ are specified correctly and $(X,M)$ follows a bivariate normal distribution, i.e. $(X,M) \sim N_2\left(\mu_X, \mu_M, \sigma_X^2, \sigma_M^2, \rho\right)$. However, in real life applications, these assumptions may not always hold and whether the performance of the control chart is adversely affected when these assumptions are violated is of interest especially to quality practitioners. Hence, in this section, the robustness of the VP-AI chart is studied by evaluating its performance in terms of $ATS_1$ when there are violations in these assumptions. As can be seen in the preceding sections, the EWMA-AI chart is the only competing chart that challenges the performance of the VP-AI chart (especially for small shifts for which the EWMA-AI chart is known to be sensitive). Thus, the robustness of the VP-AI chart is compared with the EWMA-AI chart for two cases when the assumptions are violated which are (i) misspecifications in the value of $\rho$, or (ii) $(X,M)$ does not follow a bivariate normal distribution.

### 6.1 Comparative studies of the VP-AI chart under the misspecifications of $\rho$

This section presents the performance comparison between the VP-AI and EWMA-AI charts when $\rho$ is misspecified even though $(X,M) \sim N_2\left(\mu_X, \mu_M, \sigma_X^2, \sigma_M^2, \rho\right)$. Table 8 shows the $ATS_1$ values of the VP-AI and EWMA-AI charts for $\rho_{\text{miss}} \in \{0.3,\ 0.7\}$, $t_S = 0.01$, $\text{ATS}_0 = 370$, $n_0 \in \{5,7\}$, $\rho \in \{0.25, 0.5, 0.75, 0.9, 0.95\}$ and $\delta \in \{0.2, 0.4, 0.6, 0.8, 1, 1.5, 2\}$. Note that $\rho_{\text{miss}}$ denotes the misspecified value of $\rho$. To compute the $ATS_1$ values of the VP-AI chart when $\rho$ is misspecified, the optimal parameters provided in Table 1 are used but with $\rho_{\text{miss}} \in \{0.3, 0.7\}$ instead of $\rho \in \{0, 0.25, 0.5, 0.75, 0.9, 0.95\}$. For example, based on Table 1, for $n_0 = 5$, $\rho = 0.5$ and $\delta = 0.2$, the optimal parameters are $n_S = 2$, $n_L = 31$, $t_L = 1.11$, $K_2 =$

2.225, $W_1$ = 1.628 and $W_2$ = 1.527. Using the same optimal parameters, the value of $\rho$ = 0.5 is changed to $\rho_{\text{miss}} \in \{0.3, 0.7\}$ when computing the $\text{ATS}_1$ values of the VP-AI chart. The same approach is adopted in determining the parameters of the VP-AI chart for use when $\rho \in \{0, 0.25, 0.75, 0.9, 0.95\}$. It is worth noting that, even though $\rho$ is misspecified, $\text{ATS}_0 = 370$ when $\delta$ = 0 for both VP-AI and EWMA-AI charts (same as the case when the correct value of $\rho$ is used).

-- Insert Table 8 here –

As can be seen in Table 8, for $\rho_{\text{miss}}$ = 0.3 and $n_0$ = 5, the VP-AI chart surpasses the EWMA-AI chart for all shifts, as the former has smaller $\text{ATS}_1$ values than the latter, except $\delta$ = 0.2 ($\delta \in \{0.2, 0.4\}$) for $\rho \leq 0.5$ ($\rho \geq 0.75$). Meanwhile, for $\rho_{\text{miss}}$ = 0.3 and $n_0$ = 7, the VP-AI chart is superior to the EWMA-AI chart for all shifts, except $\delta$ = 0.2 ($\delta \in \{0.2, 0.4\}$) for $\rho \in \{0.25, 0.5, 0.75, 0.95\}$ ($\rho$ = 0.9). For $\rho_{\text{miss}}$ = 0.7, the VP-AI chart is superior to the EWMA-AI chart with the exception of $\delta$ = 0.2 when $n_0 = \{5, 7\}$. To summarize, the VP-AI chart still outperforms the EWMA-AI chart for moderate and large shifts with the misspecification of $\rho$.

### 6.2 Comparative studies of the VP-AI chart under the violations of bivariate normality

In the design of AI control charts, it is usually assumed that $(X, M)$ comes from a bivariate normal distribution, which may not be true for some processes. Thus, in this section, the performance of the VP-AI chart is evaluated and compared with the EWMA-AI chart when bivariate normality is violated. To study the performance of the VP $\bar{X}$ chart under non-normality, Lin and Chou (2007) used the *t* and gamma distributions to represent non-normal symmetric and skewed distributions, respectively. Additionally, Borror et al. (1999), Calzada and Scariano (2001), and Stoumbos and Reynolds (2000) have used the gamma and *t* distributions to represent various non-normal populations when they studied the robustness of

control charts to non-normality. In this section, the bivariate non-normal distributions considered for comparing the effects of symmetric and skewed distributions on the VP-AI and EWMA-AI charts are the bivariate *t* and bivariate gamma distributions. Note that simulation is used to obtain the $ATS_1$ values, based on the assumption that $(X,M)$ comes from the bivariate *t* and bivariate gamma distributions, instead of the bivariate normal distribution. The optimal parameters adopted for the EWMA-AI and VP-AI charts are $(\lambda,k)$ = (0.21, 2.8715) and $(n_s,n_L,t_L,K_2,W_1,W_2)$ = (2, 16, 1.27, 2.4945, 1.2419, 1.2154), respectively, which are obtained by minimizing $ATS_1$ when $\delta$ = 0.5, $\rho$ = 0.5, $ATS_0$ = 370, $t_S$ = 0.01 and $n_0$ = 5, based on the bivariate normal distribution.

Table 9 shows the $ATS_1$ values of the EWMA-AI and VP-AI charts for the bivariate *t* distribution with $v \in \{3, 10, 20\}$ degrees of freedom when $\rho \in \{0.25, 0.5, 0.75, 0.9, 0.95\}$ and $\delta \in \{0, 0.2, 0.4, 0.6, 0.8, 1, 1.5, 2\}$. It can be seen in Table 9 that, as *v* increases, the $ATS_0$ value (when $\delta$ = 0) of the VP-AI and EWMA-AI charts under the bivariate *t* distribution approaches 370 (which is similar to the bivariate normal distribution that has $ATS_0$ = 370). However, the $ATS_0$ value of the VP-AI chart is larger and closer to 370 in comparison with the $ATS_0$ of the EWMA-AI chart, indicating that the VP-AI chart is more robust against a symmetric non-normal distribution. To illustrate, when $\delta$ = 0 and $\rho$ = 0.25, the $ATS_0$ values of the VP-AI and EWMA-AI charts when *v* = 3 (*v* = 20) are 284.09 (371.32) and 214.63 (356.94), respectively. It is found that $\rho$ has no influence on the charts' $ATS_0$ values but for the out-of-control case, the charts become more sensitive with an increase in $\rho$. This is because the $ATS_1$ values of both charts decrease as $\rho$ increases. For example, when *v* = 10 and $\delta$ = 0.2, the $ATS_1$ values of the VP-AI (EWMA-AI) charts decrease from 79.91 (43.23) when $\rho$ = 0.25 to 3.16 (5.48) when $\rho$ = 0.95. When $\delta$ increases, the $ATS_1$ values of both charts decrease. Additionally, when $\delta$ is small (with the exception of $\rho$ = 0.9 and 0.95),

the EWMA-AI chart is superior to the VP-AI chart but the former's superiority is at the expense of the former having substantially lower $ATS_0$ values than the latter. As for moderate to large shifts, the VP-AI chart surpasses the EWMA-AI chart. Note that the VP-AI chart outperforms the EWMA-AI chart by having smaller $ATS_1$ values for all $\delta$ (> 0) when $\rho$ = 0.95. For example, when $v \in \{3, 10, 20\}$, $\delta = 0.2$ and $\rho = 0.95$, $ATS_1 \in \{3.47, 3.16, 3.19\}$ for the VP-AI chart, while that for the EWMA-AI chart are $ATS_1 \in \{5.51, 5.48, 5.50\}$, where the former has smaller $ATS_1$ values than the latter.

-- Insert Table 9 here –

On the other hand, Table 10 shows the $ATS_1$ values of the EWMA-AI and VP-AI charts for the bivariate gamma distribution with $G(\beta, \alpha)$, where $\beta \in \{1, 2\}$ and $\alpha = 1$ when $\rho \in \{0.25, 0.5, 0.75, 0.9, 0.95\}$ and $\delta \in \{0, 0.2, 0.4, 0.6, 0.8, 1, 1.5, 2\}$. Note that for $G(\beta, \alpha)$, $\beta$ is the shape parameter and $\alpha$ is the scale parameter. It can be seen in Table 10 that, the VP-AI and EWMA-AI charts under the bivariate gamma distribution has a larger $ATS_0$ value (closer performance to the bivariate normal distribution) when $\beta$ is smaller. To illustrate, when $\delta = 0$ and $\rho = 0.5$, the $ATS_0$ values of the VP-AI and EWMA-AI charts for $G(1, 1)$ ($G(2, 1)$) distributions are 285.90 (32.53) and 200.90 (31.36), respectively. For $G(1, 1)$, the $ATS_0$ value of the VP-AI chart is generally larger and closer to 370 in comparison with the corresponding $ATS_0$ value of the EWMA-AI chart, indicating that the VP-AI chart is more robust against a skewed non-normal distribution. However, for $G(2, 1)$, both VP-AI and EWMA-AI charts show a lack of robustness as their $ATS_0$ values are far from the designed value of 370.

Still investigating Table 10, it is seen that an increase in the value of $\rho$ decreases the charts' $ATS_0$ value which explains why the charts become more sensitive for the out-of-control case when $\rho$ increases. The $ATS_1$ values of both charts decrease as $\rho$ increases. As an example, for $G(1, 1)$ and $\delta = 0.2$, the $ATS_1$ values of the VP-AI (EWMA-AI) charts decrease

from 90.25 (37.28) when $\rho$ = 0.25 to 6.24 (5.63) when $\rho$ = 0.95. It is found that the VP-AI chart always has a higher $ATS_0$ value than the EWMA-AI chart when $\rho$ is fixed. For example, for $G(1, 1)$, $ATS_0 \in \{393.10\ (249.40), 285.90\ (200.90), 177.64\ (128.61), 112.42\ (81.43), 97.06\ (66.18)\}$ when $\rho \in \{0.25, 0.5, 0.75, 0.9, 0.95\}$ for the VP-AI (EWMA-AI) charts. When $\delta$ increases, the $ATS_1$ values of both charts decrease. Additionally, when $\delta$ is small (with the exception of $\rho$ = 0.95 for $G(2, 1)$), the EWMA-AI chart is superior to the VP-AI chart but the former's superiority is at the expense of the former having generally lower $ATS_0$ values than the latter. As for moderate to large shifts, the VP-AI chart surpasses the EWMA-AI chart. For example, for $G(1, 1)$ when $\rho$ = 0.5 and $\delta$ = 0.6, the VP-AI chart outperforms the EWMA-AI chart as the former's $ATS_1$ = 3.56, which is lower than the latter's $ATS_1$ = 5.08.

-- Insert Table 10 here –

**7. An illustrative example**

An example that illustrates the implementation of the VP-AI chart is given in this section using the dataset on a spring manufacturing process taken from Chen, Cheng, and Xie (2005) and adopted by Ghute and Shirke (2008). In a spring manufacturing process, the spring elasticity represents the study variable $X$ that is monitored for process shifts. Meanwhile, the spring inner diameter represents the auxiliary variable $M$ which is correlated to $X$ and $(X, M)$ follows a bivariate normal distribution. As the exact shift size $\delta$ for which a quick detection is needed cannot be specified a priori by the quality engineer, the optimal parameters of the VP-AI chart are obtained by minimizing $EATS_1$ for the range of shifts $(\delta_{\min}, \delta_{\max}) = (1, 1.5)$ with the assumption that $\delta$ follows a uniform distribution over the range $(\delta_{\min}, \delta_{\max})$, i.e. $\delta \sim U(1, 1.5)$.

According to the historical Phase-I dataset given in Chen et al. (2005), the correlation coefficient, as well as the in-control means and standard deviations of $X$ and $M$ are given by $\rho = -0.5172,\ \mu_{X0} = 45.85,\ \mu_M = 28.29,\ \sigma_X = 0.1503$ and $\sigma_M = 0.0592$. Using the optimization algorithm outlined in Section 3.3 with the constraints $\mathrm{ASS}_0 = 5,\ \mathrm{ASI}_0 = 1$ and $\mathrm{ATS}_0 = 370,$ the optimal parameters $(n_S, n_L, t_S, t_L, K_1, K_2, W_1, W_2) =$ (3, 6, 0.1, 2.8, 6, 2.874, 0.431, 0.429) are obtained. Table 11 shows the bivariate observations $(X, M)$, charting statistic $Z_r$, sampling interval and total time elapsed for 19 samples. Additionally, Figure 2 shows the application of the VP-AI chart on the spring manufacturing process dataset. The points plotted on the VP-AI chart are the charting statistics, $Z_r$, for $r$ = 1, 2, …, 19, from Table 11. The parameters of the VP-AI chart that can be varied are the sample size, sampling interval, as well as control and warning limits that vary according to the location of the previous $Z_r$ statistic plotted on the VP-AI chart. Note that each sample can either be small $(n_S = 3)$ and taken after a long $(t_L = 2.8 \text{ hours})$ sampling interval or large $(n_L = 6)$ and taken after a short $(t_S = 0.1 \text{ hours})$ sampling interval. To relax the control, loosened control and warning limits $(K_1, -K_1, W_1, -W_1) = (6, -6, 0.431, -0.431)$ are adopted with the parameters $(n_S, t_L)$. On the other hand, to tighten the control, tightened control and warning limits $(K_2, -K_2, W_2, -W_2) = (2.874, -2.874, 0.429, -0.429)$ are adopted with the parameters $(n_L, t_S)$. Table 11 can be interpreted as follows:

- For the first sample $(r = 1)$, process monitoring begins with the assumption that a small sample of size $n_S = 3$ is taken after a long sampling interval $t_L = 2.8$ hours, with loosened control and warning limits $(K_1, -K_1, W_1, -W_1) = (6, -6, 0.431, -0.431)$.

- Then $Z_1$ = 1.0908 is computed using Equation (4). As $Z_1 = 1.0908 \in I_2$ (warning region) indicates that there is a higher tendency for the process to shift to an out-of-control condition, the control for the second sample $(r = 2)$ is tightened. Hence, for the second sample, the parameters $(n_L, t_S) = (6, 0.1)$ and $(K_2, -K_2, W_2, -W_2) = (2.874, -2.874, 0.429, -0.429)$ are adopted to tighten the control.
- On the other hand, for the fourth sample $(r = 4)$, as $Z_4 = -0.2026 \in I_1$ (central region) implies that there is a lower possibility for the process to be out-of-control, the control for the fifth sample $(r = 5)$ is relaxed. Thus, the parameters $(n_S, t_L) = (3, 2.8)$ and $(K_1, -K_1, W_1, -W_1) = (6, -6, 0.431, -0.431)$ are adopted to relax the control.
- At the 15th sample ($r$ = 15), $Z_{15} \in I_2$ (warning region), hence, the tightened limits $(K_2, -K_2, W_2, -W_2) = (2.874, -2.874, 0.429, -0.429)$ are adopted to evaluate sample 16. Consequently, the VP-AI chart signals an out-of-control condition at the 16th sample $(r = 16)$ as $Z_{16} = 2.9287 \in I_3$ = $(-\infty, -2.874) \cup (2.874, \infty)$ (out-of-control region). Subsequently, corrective actions are taken by the quality practitioners to remove the assignable cause(s) and return the process to its in-control condition. The total time elapsed until the VP-AI chart signals an out-of-control condition is 20.5 hours.

--Insert Table 11 here--

-- Insert Figure 2 here --

## 8. Conclusions

In control charting literature, researchers strive to improve the sensitivity of control charts in order to enhance the effectiveness of control charts in quality and process monitoring.

Control charts that incorporate auxiliary information have been shown to vastly improve quality and process monitoring in the literature. Hence, in this paper, the VP-AI chart with improved effectiveness in monitoring process mean is developed through the incorporation of the auxiliary information approach with the VP control charting scheme. By employing a regression estimator of the process mean that incorporates information from the study and auxiliary variables, process monitoring has vastly improved. Consequently, the VP-AI chart outperforms the standard VP chart for all values of shifts; thus, justifying the integration of auxiliary information. The VP-AI chart involves parameters (sample size, sampling interval, control and warning limits) that can be varied according to the location of the previous sample statistic plotted on the chart.

The VP-AI chart is studied and subsequently compared with five existing AI charts which are the SH-AI, SYN-AI, EWMA-AI, RS-AI and VSSI-AI charts. The charts are compared in terms of $ATS_1$ and $SDTS_1$ when the exact shift size can be specified a priori and $EATS_1$ when the exact shift size cannot be specified in advance. The VP-AI chart significantly outperforms the SH-AI, SYN-AI and VSSI-AI charts for all levels of shifts. Meanwhile, the VP-AI chart outperforms the EWMA-AI and RS-AI charts for most shifts. Additionally, the VP-AI chart has a lower spread in the time to signal distribution in comparison with the SH-AI, SYN-AI, RS-AI and VSSI-AI charts for small and moderate shifts. Thus, this justifies the development of the VP-AI chart as an enhanced control charting scheme that has a better ability to monitor the process mean. Owing to the enhanced process monitoring performance of the proposed VP-AI chart in comparison to the standard VP and five existing AI charts, the proposed chart will be a useful approach to quality practitioners in monitoring the process mean and significantly contributes to the present literature of AI charts. This paper also studies the robustness of the VP-AI chart by examining and comparing its performance with the EWMA-AI chart under misspecifications of $\rho$ and

violation of bivariate normality. Overall, it is found that the VP-AI chart is more robust than the EWMA-AI chart when the size of the shift is moderate or large.

The implementation of the VP-AI chart is illustrated with a dataset from a spring manufacturing process in this paper to provide a better understanding of the workings of the VP-AI chart. As the VP-AI chart that monitors process mean is proposed in this paper, future research can consider its VP-AI counterpart that monitors the process variance. A future extension that studies the performance of the VP-AI chart when process parameters are estimated can also be explored. In this paper, only one auxiliary variable is used. Additionally, the economic design of the VP-AI chart can be studied as a future research. The adaptive EWMA or RS charts that incorporate the auxiliary information method can also be considered in future research works.

**Acknowledgements**

This research is supported by the Kementerian Pendidikan Malaysia, Fundamental Research Grant Scheme, number 203.PMATHS.6711603.

**List of Acronyms**

| | |
|---|---|
| AI | auxiliary information |
| ARL | average run length |
| $ASI_0$ | in-control average sampling interval |
| $ASS_0$ | in-control average sample size |
| ATS | average time to signal |
| $ATS_0$ | in-control ATS |
| $ATS_1$ | out-of-control ATS |
| CV | coefficient of variation |

| | |
|---|---|
| EATS | expected average time to signal |
| $EATS_0$ | in-control EATS |
| $EATS_1$ | out-of-control EATS |
| EWMA | exponentially weighted moving average |
| EWMA-AI | EWMA with auxiliary information |
| RS | run sum |
| RS-AI | RS with auxiliary information |
| SDTS | standard deviation of the time to signal |
| $SDTS_1$ | out-of-control SDTS |
| SH-AI | Shewhart with auxiliary information |
| SYN-AI | synthetic with auxiliary information |
| tpm | transition probability matrix |
| VSS | variable sample size |
| VSI | variable sampling interval |
| VSSI | variable sample size and sampling interval |
| VSSI-AI | VSSI with auxiliary information |
| VP | variable parameters |
| VP-AI | VP with auxiliary information |

**References**

Abbas, N., M. Riaz, and R. J. M. M. Does. 2014. An EWMA-type control chart for monitoring the process mean using auxiliary information. *Communications in Statistics - Theory and Methods*, 43(16): 3485-3498.

Abbasi, S. A., and M. Riaz. 2016. On dual use of auxiliary information for efficient monitoring. *Quality and Reliability Engineering International*, 32(2): 705-714.

Ahmad, S., S. A. Abbasi, M. Riaz, and N. Abbas. 2014. On efficient use of auxiliary information for control charting in SPC. *Computers & Industrial Engineering*, *67*, 173-184.

Borror, C. M., D. C. Montgomery, and G. C. Runger. 1999. Robustness of the EWMA control chart to non-normality. *Journal of Quality Technology*, 31(3): 309-316.

Bourke, P. D. 2020. Detecting a downward shift in a proportion using a geometric CUSUM chart. *Quality Engineering*, 32(1): 75-90.

Calzada, M. E., and S. M. Scariano. 2001. The robustness of the synthetic control chart to non-normality. *Communications in Statistics - Simulation and Computation*, 30(2): 311-326.

Carot, V., J. M. Jabaloyes, and T. Carot. 2002. Combined double sampling and variable sampling interval $\bar{X}$ chart. *International Journal of Production Research*, 40(9): 2175-2186.

Castagliola, P., A. Achouri, H. Taleb, G. Celano, and S. Psarakis. 2013. Monitoring the coefficient of variation using a variable sampling interval control chart. *Quality and Reliability Engineering International*, 29(8): 1135-1149.

Chen, Y. K., and H. H. Chang. 2008. Economic design of variable parameters $\bar{X}$ control charts for processes with fuzzy mean shifts. *Journal of the Operational Research Society*, 59(8): 1128-1135.

Chen, G., S. W. Cheng, and H. Xie. 2005. A new multivariate control chart for monitoring both location and dispersion. *Communications in Statistics - Simulation and Computation*, 34(1): 203-217.

Chong, N. L., M. B. C. Khoo, A. Haq, and P. Castagliola. 2019. Hotelling's $T^2$ control charts with fixed and variable sample sizes for monitoring short production runs. *Quality and Reliability Engineering International*, 35(1): 14-29.

Chong, Z. L., A. Mukherjee, and M. B. C. Khoo. 2020. Some simplified Shewhart-type distribution-free joint monitoring schemes and its application in monitoring drinking water turbidity. *Quality Engineering*, 32(1): 91-110.

Costa, A. F. B. 1994. $\bar{X}$ charts with variable sample size. *Journal of Quality Technology*, 26(3): 155-163.

Costa, A. F. B. 1999. $\bar{X}$ charts with variable parameters. *Journal of Quality Technology*, 31(4): 408-416.

Ghute, V. B., and D. T. Shirke. 2008. A multivariate synthetic control chart for monitoring process mean vector. *Communications in Statistics - Theory and Methods*, 37(13): 2136-2148.

Guo, Z. F., L. S. Cheng, and Z. D. Lu. 2014. Economic Design of the Variable Parameters Control Chart with a Corrected A&L Switching Rule. *Quality and Reliability Engineering International*, 30(2): 235-246.

Haq, A., and M. B. C. Khoo. 2016. A new synthetic control chart for monitoring process mean using auxiliary information. *Journal of Statistical Computation and Simulation*, 86(15): 3068-3092.

Hu, X., P. Castagliola, J. Sun, and M. B. C. Khoo. 2016. The performance of variable sample size chart with measurement errors. *Quality and Reliability Engineering International*, 32(3): 969-983.

Khatun, M., M. B. C. Khoo, M. H. Lee, and P. Castagliola. 2019. One-sided control charts for monitoring the multivariate coefficient of variation in short production runs. *Transactions of the Institute of Measurement and Control*, 41(6): 1712-1728.

Khoo, M. B. C., M. Y. See, N. L. Chong, and W. L. Teoh. 2019. An improved variable sample size and sampling interval *S* control chart. *Quality and Reliability Engineering International*, 35(1): 392-404.

Lawson, J. 2019. Phase II monitoring of variability using Cusum and EWMA charts with individual observations. *Quality Engineering*, 31(3): 417-429.

Lee, H., M. Aslam, Q. U. Shakeel, W. Lee, and C. H. Jun. 2015. A control chart using an auxiliary variable and repetitive sampling for monitoring process mean. *Journal of Statistical Computation and Simulation*, 85(16): 3289-3296.

Lee, M. H., and M. B. C. Khoo. 2018. Double sampling |**S**| control chart with variable sample size and variable sampling interval. *Communications in Statistics - Simulation and Computation*, 47(2): 615-628.

Lin, Y. C., and C. Y. Chou. 2007. Non-normality and the variable parameters $\bar{X}$ control charts. *European Journal of Operational Research*, 176(1): 361-373.

Mahadik, S. B., and D. T. Shirke. 2009. A special variable sample size and sampling interval chart. *Communications in Statistics - Theory and Methods*, 38(8): 1284-1299.

Mandel, B. J. (1969). The regression control chart. *Journal of Quality Technology*, 1(1): 1-9.

Mehmood, R., M. H. Lee, S. Hussain, and M. Riaz. 2019. On efficient construction and evaluation of runs rules–based control chart for known and unknown parameters under different distributions. *Quality and Reliability Engineering International*, 35(2): 582-599.

Ng, P. S., M. B. C. Khoo, S. Saha, and S. Y. Teh. 2018. Run Sum Chart for the Mean with Auxiliary Information. *Journal of Testing and Evaluation*, 48(2): 1554-1575.

Prabhu, S. S., D. C. Montgomery, and G. C. Runger. 1994. A combined adaptive sample size and sampling interval $\bar{X}$ control scheme. *Journal of Quality Technology*, 26(3): 164-176.

Psarakis, S. (2015). Adaptive control charts: recent developments and extensions. *Quality and Reliability Engineering International*, 31(7): 1265-1280.

Reynolds, M. R., R. W. Amin, J. C. Arnold, and J. C. Nachlas. 1988. Charts with variable sampling intervals. Technometrics, 30(2): 181-192.

Riaz, M. 2008. Monitoring process mean level using auxiliary information. *Statistica Neerlandica*, 62(4): 458-481.

Riaz, M. 2011. An improved control chart structure for process location parameter. *Quality and Reliability Engineering International*, 27(8): 1033-1041.

Riaz, M., R. Mehmood, S. Ahmad, and S. A. Abbasi. 2013. On the performance of auxiliary-based control charting under normality and nonnormality with estimation effects. *Quality and Reliability Engineering International*, 29(8): 1165-1179.

Saha, S., M. B. C. Khoo, M. H. Lee, and A. Haq. 2019. A variable sample size and sampling interval control chart for monitoring the process mean using auxiliary information. *Quality Technology & Quantitative Management*, 16(4): 389-406.

Shu, L., F. Tsung, and K. L. Tsui. 2005. Effects of estimation errors on cause-selecting charts. *IIE Transactions*, 37(6): 559-567.

Sparks, R. S. 2000. CUSUM charts for signalling varying location shifts. *Journal of Quality Technology*, 32(2): 157-171.

Stoumbos, Z. G. B., and M. R. Reynolds Jr. 2000. Robustness to non-normality and autocorrelation of individuals control charts. *Journal of Statistical Computation and Simulation*, 66(2): 145-187.

Tagaras, G. (1998). A survey of recent developments in the design of adaptive control charts. *Journal of Quality Technology*, 30(3): 212-231.

Wade, M. R., and W. H. Woodall. 1993. A review and analysis of cause-selecting control charts. *Journal of Quality Technology*, 25(3): 161-169.

Wang, R. F., X. Fu, J. C. Yuan, and Z. Y. Dong. 2018. Economic design of variable-parameter $\bar{X}$-Shewhart control chart used to monitor continuous production. *Quality Technology & Quantitative Management*, 15(1): 106-124.

Yeong, W. C., S. L. Lim, M. B. C. Khoo, and P. Castagliola. 2018. Monitoring the coefficient of variation using a variable parameters chart. *Quality Engineering*, 30(2): 212-235.

Zhang, G. X. (1985). Cause-selecting control charts - a new type of quality control charts. *The QR Journal*, *12*(4): 221-225.

Table 1. Optimal parameters, $ATS_1$ and $SDTS_1$ values of the VP-AI chart, for $t_s = 0.01$, $ATS_0 = 370$, $n_0 \in \{5, 7\}$, $\rho \in \{0, 0.25, 0.5, 0.75, 0.9, 0.95\}$ and $\delta \in \{0.2, 0.4, 0.6, 0.8, 1, 1.5, 2\}$

| $n_0 = 5$ |
|---|

| | $n_S$ | $n_L$ | $t_L$ | $K_2$ | $W_1$ | $W_2$ | $ATS_1$ | $SDTS_1$ | $n_S$ | $n_L$ | $t_L$ | $K_2$ | $W_1$ | $W_2$ | $ATS_1$ | $SDTS_1$ | $n_S$ | $n_L$ | $t_L$ | $K_2$ | $W_1$ | $W_2$ | $ATS_1$ | $SDTS_1$ |
|---|---|---|---|---|---|---|---|---|---|---|---|---|---|---|---|---|---|---|---|---|---|---|---|---|
| $\delta$ | | | | $\rho = 0$ | | | | | | | | $\rho = 0.25$ | | | | | | | | $\rho = 0.5$ | | | | |
| 0.2 | 2 | 31 | 1.11 | 2.225 | 1.628 | 1.527 | 55.28 | 55.63 | 2 | 31 | 1.11 | 2.225 | 1.628 | 1.527 | 51.37 | 51.72 | 2 | 31 | 1.11 | 2.225 | 1.628 | 1.527 | 39.43 | 39.76 |
| 0.4 | 2 | 30 | 1.12 | 2.238 | 1.611 | 1.516 | 9.75 | 9.89 | 2 | 28 | 1.13 | 2.267 | 1.574 | 1.491 | 9.02 | 9.17 | 2 | 23 | 1.17 | 2.348 | 1.465 | 1.408 | 6.89 | 7.01 |
| 0.6 | 2 | 15 | 1.30 | 2.521 | 1.198 | 1.176 | 3.64 | 3.74 | 2 | 14 | 1.33 | 2.549 | 1.150 | 1.131 | 3.37 | 3.48 | 2 | 12 | 1.42 | 2.612 | 1.036 | 1.023 | 2.60 | 2.72 |
| 0.8 | 2 | 9 | 1.74 | 2.732 | 0.792 | 0.786 | 1.91 | 2.13 | 3 | 9 | 1.50 | 2.648 | 0.967 | 0.957 | 1.80 | 1.75 | 3 | 7 | 1.99 | 2.782 | 0.675 | 0.670 | 1.46 | 1.62 |
| 1 | 3 | 7 | 1.99 | 2.782 | 0.675 | 0.670 | 1.30 | 1.43 | 3 | 6 | 2.98 | 2.874 | 0.431 | 0.429 | 1.25 | 1.76 | 3 | 6 | 2.98 | 2.874 | 0.431 | 0.429 | 1.12 | 1.59 |
| 1.5 | 4 | 6 | 1.99 | 2.782 | 0.670 | 0.675 | 1.02 | 1.02 | 4 | 6 | 1.99 | 2.782 | 0.675 | 0.670 | 1.00 | 1.01 | 4 | 6 | 1.99 | 2.782 | 0.675 | 0.670 | 1.00 | 1.00 |
| 2 | 3 | 6 | 2.98 | 2.874 | 0.431 | 0.429 | 1.00 | 1.41 | 3 | 6 | 2.98 | 2.874 | 0.431 | 0.429 | 1.00 | 1.41 | 3 | 6 | 2.98 | 2.874 | 0.431 | 0.429 | 1.00 | 1.41 |
| $\delta$ | | | | $\rho = 0.75$ | | | | | | | | $\rho = 0.9$ | | | | | | | | $\rho = 0.95$ | | | | |
| 0.2 | 2 | 31 | 1.11 | 2.225 | 1.628 | 1.527 | 19.74 | 19.99 | 2 | 24 | 1.16 | 2.330 | 1.490 | 1.427 | 7.00 | 7.12 | 2 | 13 | 1.37 | 2.579 | 1.097 | 1.080 | 3.11 | 3.24 |
| 0.4 | 2 | 15 | 1.30 | 2.521 | 1.198 | 1.176 | 3.57 | 3.67 | 3 | 7 | 1.99 | 2.782 | 0.674 | 0.670 | 1.48 | 1.64 | 3 | 6 | 2.98 | 2.874 | 0.431 | 0.429 | 1.06 | 1.51 |
| 0.6 | 3 | 8 | 1.66 | 2.710 | 0.842 | 0.834 | 1.51 | 1.51 | 4 | 6 | 1.99 | 2.782 | 0.674 | 0.670 | 1.03 | 1.04 | 3 | 6 | 2.98 | 2.874 | 0.431 | 0.429 | 1.00 | 1.41 |
| 0.8 | 3 | 6 | 2.98 | 2.874 | 0.431 | 0.429 | 1.09 | 1.55 | 3 | 6 | 2.98 | 2.874 | 0.431 | 0.429 | 1.00 | 1.41 | 2 | 6 | 3.97 | 2.911 | 0.319 | 0.317 | 1.00 | 1.72 |
| 1 | 4 | 6 | 1.99 | 2.782 | 0.674 | 0.670 | 1.02 | 1.02 | 3 | 6 | 2.98 | 2.874 | 0.431 | 0.429 | 1.00 | 1.41 | 4 | 6 | 1.99 | 2.782 | 0.674 | 0.670 | 1.00 | 0.99 |
| 1.5 | 3 | 6 | 2.98 | 2.874 | 0.431 | 0.429 | 1.00 | 1.41 | 4 | 6 | 1.99 | 2.782 | 0.674 | 0.670 | 1.00 | 0.99 | 4 | 6 | 1.99 | 2.782 | 0.674 | 0.670 | 1.00 | 0.99 |
| 2 | 4 | 6 | 1.99 | 2.782 | 0.674 | 0.670 | 1.00 | 0.99 | 4 | 6 | 1.99 | 2.782 | 0.674 | 0.670 | 1.00 | 0.99 | 4 | 6 | 1.99 | 2.782 | 0.674 | 0.670 | 1.00 | 0.21 |
| $n_0 = 7$ | | | | | | | | | | | | | | | | | | | | | | | | |
| $\delta$ | | | | $\rho = 0$ | | | | | | | | $\rho = 0.25$ | | | | | | | | $\rho = 0.5$ | | | | |
| 0.2 | 2 | 31 | 1.21 | 2.417 | 1.364 | 1.324 | 43.42 | 43.85 | 2 | 31 | 1.21 | 2.417 | 1.364 | 1.324 | 39.98 | 40.41 | 2 | 31 | 1.21 | 2.417 | 1.364 | 1.324 | 29.67 | 30.08 |
| 0.4 | 2 | 31 | 1.21 | 2.417 | 1.364 | 1.324 | 6.39 | 6.62 | 2 | 29 | 1.23 | 2.443 | 1.325 | 1.290 | 5.92 | 6.15 | 2 | 24 | 1.29 | 2.516 | 1.207 | 1.184 | 4.55 | 4.78 |
| 0.6 | 3 | 16 | 1.44 | 2.621 | 1.020 | 1.007 | 2.46 | 2.55 | 3 | 15 | 1.50 | 2.648 | 0.967 | 0.957 | 2.29 | 2.40 | 3 | 12 | 1.79 | 2.744 | 0.765 | 0.759 | 1.82 | 2.03 |
| 0.8 | 4 | 10 | 1.99 | 2.782 | 0.674 | 0.670 | 1.40 | 1.57 | 4 | 9 | 2.49 | 2.841 | 0.524 | 0.522 | 1.34 | 1.70 | 4 | 8 | 3.97 | 2.911 | 0.319 | 0.317 | 1.17 | 1.98 |
| 1 | 5 | 8 | 2.98 | 2.874 | 0.431 | 0.429 | 1.10 | 1.54 | 5 | 8 | 2.98 | 2.874 | 0.431 | 0.429 | 1.07 | 1.51 | 5 | 8 | 2.98 | 2.874 | 0.431 | 0.429 | 1.03 | 1.45 |
| 1.5 | 5 | 8 | 2.98 | 2.874 | 0.431 | 0.429 | 1.00 | 1.41 | 5 | 8 | 2.98 | 2.874 | 0.431 | 0.429 | 1.00 | 1.41 | 4 | 8 | 3.97 | 2.911 | 0.319 | 0.317 | 1.00 | 1.72 |
| 2 | 3 | 8 | 4.96 | 2.931 | 0.253 | 0.252 | 1.00 | 1.99 | 3 | 8 | 4.96 | 2.931 | 0.253 | 0.252 | 1.00 | 1.99 | 3 | 8 | 4.96 | 2.931 | 0.253 | 0.252 | 1.00 | 1.99 |
| $\delta$ | | | | $\rho = 0.75$ | | | | | | | | $\rho = 0.9$ | | | | | | | | $\rho = 0.95$ | | | | |
| 0.2 | 2 | 31 | 1.21 | 2.417 | 1.364 | 1.324 | 13.63 | 13.98 | 2 | 24 | 1.29 | 2.516 | 1.207 | 1.184 | 4.62 | 4.86 | 3 | 14 | 1.57 | 2.677 | 0.908 | 0.900 | 2.13 | 2.27 |
| 0.4 | 3 | 15 | 1.50 | 2.648 | 0.967 | 0.957 | 2.42 | 2.54 | 4 | 8 | 3.97 | 2.911 | 0.319 | 0.317 | 1.18 | 1.99 | 5 | 8 | 2.98 | 2.874 | 0.431 | 0.429 | 1.01 | 1.43 |
| 0.6 | 4 | 8 | 3.97 | 2.911 | 0.319 | 0.317 | 1.19 | 2.01 | 5 | 8 | 2.98 | 2.874 | 0.431 | 0.429 | 1.01 | 1.42 | 4 | 8 | 3.97 | 2.911 | 0.319 | 0.317 | 1.00 | 1.72 |
| 0.8 | 5 | 8 | 2.98 | 2.874 | 0.431 | 0.429 | 1.02 | 1.44 | 4 | 8 | 3.97 | 2.911 | 0.319 | 0.317 | 1.00 | 1.72 | 3 | 8 | 4.96 | 2.931 | 0.253 | 0.252 | 1.00 | 1.99 |
| 1 | 5 | 8 | 2.98 | 2.874 | 0.431 | 0.429 | 1.00 | 1.41 | 3 | 8 | 4.96 | 2.931 | 0.253 | 0.252 | 1.00 | 1.99 | 6 | 8 | 1.99 | 2.782 | 0.674 | 0.670 | 1.00 | 0.99 |
| 1.5 | 3 | 8 | 4.96 | 2.931 | 0.253 | 0.252 | 1.00 | 1.99 | 6 | 8 | 1.99 | 2.782 | 0.674 | 0.670 | 1.00 | 0.99 | 6 | 8 | 1.99 | 2.782 | 0.674 | 0.670 | 1.00 | 0.21 |
| 2 | 6 | 8 | 1.99 | 2.782 | 0.674 | 0.670 | 1.00 | 0.99 | 6 | 8 | 1.99 | 2.782 | 0.674 | 0.670 | 1.00 | 0.21 | 2 | 5 | 1.13 | 2.274 | 1.565 | 1.484 | 1.00 | 0.38 |

Table 2. Optimal parameters, $ATS_1$ and $SDTS_1$ values of the VP-AI chart, for $t_s = 0.1$, $ATS_0 = 370$, $n_0 \in \{5, 7\}$, $\rho \in \{0, 0.25, 0.5, 0.75, 0.9, 0.95\}$ and $\delta \in \{0.2, 0.4, 0.6, 0.8, 1, 1.5, 2\}$

| $n_0 = 5$ |
|---|

| | $n_S$ | $n_L$ | $t_L$ | $K_2$ | $W_1$ | $W_2$ | $ATS_1$ | $SDTS_1$ | $n_S$ | $n_L$ | $t_L$ | $K_2$ | $W_1$ | $W_2$ | $ATS_1$ | $SDTS_1$ | $n_S$ | $n_L$ | $t_L$ | $K_2$ | $W_1$ | $W_2$ | $ATS_1$ | $SDTS_1$ |
|---|---|---|---|---|---|---|---|---|---|---|---|---|---|---|---|---|---|---|---|---|---|---|---|---|
| $\delta$ | | | | | $\rho = 0$ | | | | | | | | $\rho = 0.25$ | | | | | | | | $\rho = 0.5$ | | | |
| 0.2 | 2 | 31 | 1.10 | 2.225 | 1.628 | 1.527 | 55.44 | 55.40 | 2 | 31 | 1.10 | 2.225 | 1.628 | 1.527 | 51.53 | 51.77 | 2 | 31 | 1.10 | 2.225 | 1.628 | 1.527 | 39.58 | 39.79 |
| 0.4 | 2 | 30 | 1.11 | 2.238 | 1.611 | 1.516 | 9.84 | 9.87 | 2 | 29 | 1.11 | 2.252 | 1.593 | 1.504 | 9.12 | 9.14 | 2 | 24 | 1.14 | 2.330 | 1.489 | 1.427 | 6.99 | 6.98 |
| 0.6 | 2 | 16 | 1.25 | 2.495 | 1.242 | 1.215 | 3.77 | 3.71 | 2 | 15 | 1.27 | 2.521 | 1.198 | 1.176 | 3.50 | 3.44 | 2 | 12 | 1.39 | 2.612 | 1.036 | 1.023 | 2.75 | 2.70 |
| 0.8 | 3 | 10 | 1.36 | 2.595 | 1.068 | 1.053 | 2.07 | 1.83 | 3 | 10 | 1.36 | 2.595 | 1.068 | 1.053 | 1.95 | 1.70 | 3 | 8 | 1.60 | 2.709 | 0.842 | 0.834 | 1.61 | 1.44 |
| 1 | 3 | 8 | 1.60 | 2.709 | 0.842 | 0.834 | 1.44 | 1.25 | 3 | 7 | 1.90 | 2.782 | 0.674 | 0.670 | 1.38 | 1.33 | 3 | 7 | 1.90 | 2.782 | 0.674 | 0.670 | 1.24 | 1.17 |
| 1.5 | 3 | 6 | 2.80 | 2.874 | 0.431 | 0.429 | 1.08 | 1.36 | 3 | 6 | 2.80 | 2.874 | 0.431 | 0.429 | 1.07 | 1.35 | 3 | 6 | 2.80 | 2.874 | 0.431 | 0.429 | 1.05 | 1.33 |
| 2 | 2 | 6 | 3.70 | 2.911 | 0.319 | 0.317 | 1.03 | 1.62 | 2 | 6 | 3.70 | 2.911 | 0.319 | 0.317 | 1.03 | 1.61 | 2 | 6 | 3.70 | 2.911 | 0.319 | 0.317 | 1.03 | 1.61 |
| $\delta$ | | | | | $\rho = 0.75$ | | | | | | | | $\rho = 0.9$ | | | | | | | | $\rho = 0.95$ | | | |
| 0.2 | 2 | 31 | 1.10 | 2.225 | 1.628 | 1.527 | 19.86 | 20.00 | 2 | 24 | 1.14 | 2.330 | 1.489 | 1.427 | 7.11 | 7.10 | 2 | 14 | 1.30 | 2.549 | 1.150 | 1.131 | 3.25 | 3.19 |
| 0.4 | 2 | 15 | 1.27 | 2.521 | 1.198 | 1.176 | 3.70 | 3.65 | 3 | 9 | 1.45 | 2.648 | 0.967 | 0.957 | 1.63 | 1.39 | 3 | 6 | 2.80 | 2.874 | 0.431 | 0.429 | 1.15 | 1.42 |
| 0.6 | 3 | 9 | 1.45 | 2.648 | 0.967 | 0.957 | 1.66 | 1.42 | 3 | 6 | 2.80 | 2.874 | 0.431 | 0.429 | 1.11 | 1.38 | 2 | 6 | 3.70 | 2.911 | 0.319 | 0.317 | 1.04 | 1.62 |
| 0.8 | 3 | 6 | 2.80 | 2.874 | 0.431 | 0.429 | 1.19 | 1.46 | 2 | 6 | 3.70 | 2.911 | 0.319 | 0.317 | 1.04 | 1.63 | 2 | 6 | 3.70 | 2.911 | 0.319 | 0.317 | 1.03 | 1.60 |
| 1 | 3 | 6 | 2.80 | 2.874 | 0.431 | 0.429 | 1.08 | 1.35 | 2 | 6 | 3.70 | 2.911 | 0.319 | 0.317 | 1.03 | 1.61 | 4 | 6 | 1.90 | 2.782 | 0.674 | 0.670 | 1.02 | 0.92 |
| 1.5 | 2 | 6 | 3.70 | 2.911 | 0.319 | 0.317 | 1.03 | 1.61 | 4 | 6 | 1.90 | 2.782 | 0.674 | 0.670 | 1.01 | 0.91 | 4 | 6 | 1.90 | 2.782 | 0.674 | 0.670 | 1.00 | 0.90 |
| 2 | 2 | 6 | 3.70 | 2.911 | 0.319 | 0.317 | 1.03 | 1.60 | 4 | 6 | 1.90 | 2.782 | 0.674 | 0.670 | 1.00 | 0.90 | 4 | 6 | 1.90 | 2.782 | 0.674 | 0.670 | 1.00 | 0.19 |
| | | | | | | | | | | | | $n_0 = 7$ | | | | | | | | | | | | |
| $\delta$ | | | | | $\rho = 0$ | | | | | | | | $\rho = 0.25$ | | | | | | | | $\rho = 0.5$ | | | |
| 0.2 | 2 | 31 | 1.19 | 2.417 | 1.364 | 1.324 | 43.68 | 43.98 | 2 | 31 | 1.19 | 2.417 | 1.364 | 1.324 | 40.24 | 40.54 | 2 | 31 | 1.19 | 2.417 | 1.364 | 1.324 | 29.91 | 30.19 |
| 0.4 | 2 | 31 | 1.19 | 2.417 | 1.364 | 1.324 | 6.50 | 6.59 | 2 | 30 | 1.20 | 2.430 | 1.345 | 1.308 | 6.04 | 6.12 | 2 | 25 | 1.25 | 2.500 | 1.233 | 1.208 | 4.68 | 4.74 |
| 0.6 | 3 | 17 | 1.36 | 2.595 | 1.068 | 1.053 | 2.61 | 2.51 | 3 | 16 | 1.40 | 2.621 | 1.020 | 1.007 | 2.44 | 2.35 | 4 | 14 | 1.39 | 2.612 | 1.036 | 1.023 | 1.97 | 1.75 |
| 0.8 | 4 | 11 | 1.68 | 2.732 | 0.792 | 0.785 | 1.55 | 1.42 | 4 | 11 | 1.68 | 2.732 | 0.792 | 0.785 | 1.48 | 1.35 | 4 | 10 | 1.90 | 2.782 | 0.674 | 0.670 | 1.30 | 1.25 |
| 1 | 4 | 9 | 2.35 | 2.841 | 0.524 | 0.522 | 1.21 | 1.33 | 4 | 9 | 2.35 | 2.841 | 0.524 | 0.522 | 1.19 | 1.31 | 4 | 8 | 3.70 | 2.911 | 0.319 | 0.317 | 1.11 | 1.67 |
| 1.5 | 3 | 8 | 4.60 | 2.931 | 0.253 | 0.252 | 1.04 | 1.86 | 3 | 8 | 4.60 | 2.931 | 0.253 | 0.252 | 1.04 | 1.86 | 3 | 8 | 4.60 | 2.931 | 0.253 | 0.252 | 1.03 | 1.85 |
| 2 | 2 | 8 | 5.50 | 2.944 | 0.210 | 0.209 | 1.02 | 2.06 | 2 | 8 | 5.50 | 2.944 | 0.210 | 0.209 | 1.02 | 2.06 | 2 | 8 | 5.50 | 2.944 | 0.210 | 0.209 | 1.02 | 2.05 |
| $\delta$ | | | | | $\rho = 0.75$ | | | | | | | | $\rho = 0.9$ | | | | | | | | $\rho = 0.95$ | | | |
| 0.2 | 2 | 31 | 1.19 | 2.417 | 1.364 | 1.324 | 13.81 | 14.01 | 2 | 25 | 1.25 | 2.500 | 1.233 | 1.208 | 4.75 | 4.82 | 3 | 15 | 1.45 | 2.648 | 0.967 | 0.957 | 2.28 | 2.21 |
| 0.4 | 3 | 17 | 1.36 | 2.595 | 1.068 | 1.053 | 2.56 | 2.47 | 4 | 10 | 1.90 | 2.782 | 0.674 | 0.670 | 1.31 | 1.26 | 4 | 8 | 3.70 | 2.911 | 0.319 | 0.317 | 1.07 | 1.64 |
| 0.6 | 4 | 10 | 1.90 | 2.782 | 0.674 | 0.670 | 1.33 | 1.27 | 4 | 8 | 3.70 | 2.911 | 0.319 | 0.317 | 1.05 | 1.62 | 2 | 8 | 5.50 | 2.944 | 0.210 | 0.209 | 1.02 | 2.07 |
| 0.8 | 4 | 8 | 3.70 | 2.911 | 0.319 | 0.317 | 1.09 | 1.65 | 3 | 8 | 4.60 | 2.931 | 0.253 | 0.252 | 1.02 | 1.85 | 2 | 8 | 5.50 | 2.944 | 0.210 | 0.209 | 1.02 | 2.05 |
| 1 | 3 | 8 | 4.60 | 2.931 | 0.253 | 0.252 | 1.04 | 1.86 | 2 | 8 | 5.50 | 2.944 | 0.210 | 0.209 | 1.02 | 2.05 | 6 | 8 | 1.90 | 2.782 | 0.674 | 0.670 | 1.00 | 0.90 |
| 1.5 | 2 | 8 | 5.50 | 2.944 | 0.210 | 0.209 | 1.02 | 2.06 | 6 | 8 | 1.90 | 2.782 | 0.674 | 0.670 | 1.00 | 0.90 | 6 | 8 | 1.90 | 2.782 | 0.674 | 0.670 | 1.00 | 0.19 |
| 2 | 6 | 8 | 1.90 | 2.782 | 0.674 | 0.670 | 1.01 | 0.90 | 6 | 8 | 1.90 | 2.782 | 0.674 | 0.670 | 1.00 | 0.64 | 6 | 31 | 1.04 | 1.828 | 2.054 | 1.622 | 1.00 | 0.35 |

Table 3. Optimal parameters and $EATS_1$ values of the VP-AI chart, for $t_s = 0.01$, $EATS_0 = 370$, $n_0 \in \{5, 7\}$, $\rho \in \{0, 0.25, 0.5, 0.75, 0.9, 0.95\}$ and

$(\delta_{\min}, \delta_{\max}) \in \{(0.2, 0.6), (0.5, 1), (1, 1.5), (1.5, 2)\}$

| | | $n_0 = 5$ | | | | | | | | | | | | | | | | | | | |
|---|---|---|---|---|---|---|---|---|---|---|---|---|---|---|---|---|---|---|---|---|---|
| | | $n_S$ | $n_L$ | $t_L$ | $K_2$ | $W_1$ | $W_2$ | $EATS_1$ | $n_S$ | $n_L$ | $t_L$ | $K_2$ | $W_1$ | $W_2$ | $EATS_1$ | $n_S$ | $n_L$ | $t_L$ | $K_2$ | $W_1$ | $W_2$ | $EATS_1$ |
| $\delta_{\min}$ | $\delta_{\max}$ | $\rho = 0$ | | | | | | | $\rho = 0.25$ | | | | | | | $\rho = 0.5$ | | | | | | |
| 0.2 | 0.6 | 2 | 31 | 1.11 | 2.225 | 1.628 | 1.527 | 15.40 | 2 | 31 | 1.11 | 2.225 | 1.628 | 1.527 | 14.28 | 2 | 31 | 1.11 | 2.225 | 1.628 | 1.527 | 11.04 |
| 0.5 | 1 | 2 | 13 | 1.37 | 2.579 | 1.097 | 1.080 | 2.78 | 2 | 12 | 1.42 | 2.612 | 1.036 | 1.023 | 2.59 | 3 | 11 | 1.33 | 2.549 | 1.150 | 1.131 | 2.06 |
| 1 | 1.5 | 3 | 6 | 2.98 | 2.874 | 0.431 | 0.429 | 1.10 | 3 | 6 | 2.98 | 2.874 | 0.431 | 0.429 | 1.08 | 3 | 6 | 2.98 | 2.874 | 0.431 | 0.429 | 1.04 |
| 1.5 | 2 | 4 | 6 | 1.99 | 2.782 | 0.675 | 0.670 | 1.01 | 4 | 6 | 1.99 | 2.782 | 0.675 | 0.670 | 1.00 | 3 | 6 | 2.98 | 2.874 | 0.431 | 0.429 | 1.00 |
| $\delta_{\min}$ | $\delta_{\max}$ | $\rho = 0.75$ | | | | | | | $\rho = 0.9$ | | | | | | | $\rho = 0.95$ | | | | | | |
| 0.2 | 0.6 | 2 | 24 | 1.16 | 2.330 | 1.490 | 1.427 | 6.05 | 2 | 13 | 1.37 | 2.579 | 1.097 | 1.080 | 2.43 | 3 | 9 | 1.50 | 2.648 | 0.967 | 0.957 | 1.37 |
| 0.5 | 1 | 3 | 7 | 1.99 | 2.782 | 0.675 | 0.670 | 1.31 | 3 | 6 | 2.98 | 2.874 | 0.431 | 0.429 | 1.02 | 3 | 6 | 2.98 | 2.874 | 0.431 | 0.429 | 1.00 |
| 1 | 1.5 | 3 | 6 | 2.98 | 2.874 | 0.431 | 0.429 | 1.00 | 2 | 6 | 3.97 | 2.911 | 0.319 | 0.317 | 1.00 | 4 | 6 | 1.99 | 2.782 | 0.675 | 0.670 | 1.00 |
| 1.5 | 2 | 2 | 6 | 3.97 | 2.911 | 0.319 | 0.317 | 1.00 | 4 | 6 | 1.99 | 2.782 | 0.675 | 0.670 | 1.00 | 4 | 6 | 1.99 | 2.782 | 0.675 | 0.670 | 1.00 |
| | | $n_0 = 7$ | | | | | | | | | | | | | | | | | | | |
| | | $n_S$ | $n_L$ | $t_L$ | $K_2$ | $W_1$ | $W_2$ | $EATS_1$ | $n_S$ | $n_L$ | $t_L$ | $K_2$ | $W_1$ | $W_2$ | $EATS_1$ | $n_S$ | $n_L$ | $t_L$ | $K_2$ | $W_1$ | $W_2$ | $EATS_1$ |
| $\delta_{\min}$ | $\delta_{\max}$ | $\rho = 0$ | | | | | | | $\rho = 0.25$ | | | | | | | $\rho = 0.5$ | | | | | | |
| 0.2 | 0.6 | 2 | 31 | 1.21 | 2.417 | 1.364 | 1.324 | 10.95 | 2 | 31 | 1.21 | 2.417 | 1.364 | 1.324 | 10.09 | 2 | 31 | 1.21 | 2.417 | 1.364 | 1.324 | 7.67 |
| 0.5 | 1 | 4 | 14 | 1.42 | 2.612 | 1.036 | 1.023 | 1.95 | 4 | 14 | 1.42 | 2.612 | 1.036 | 1.023 | 1.83 | 4 | 12 | 1.59 | 2.687 | 0.887 | 0.879 | 1.51 |
| 1 | 1.5 | 5 | 8 | 2.98 | 2.874 | 0.431 | 0.429 | 1.04 | 5 | 8 | 2.98 | 2.874 | 0.431 | 0.429 | 1.02 | 5 | 8 | 2.98 | 2.874 | 0.431 | 0.429 | 1.01 |
| 1.5 | 2 | 4 | 8 | 3.97 | 2.911 | 0.319 | 0.317 | 1.00 | 4 | 8 | 3.97 | 2.911 | 0.319 | 0.317 | 1.00 | 4 | 8 | 3.97 | 2.911 | 0.319 | 0.317 | 1.00 |
| $\delta_{\min}$ | $\delta_{\max}$ | $\rho = 0.75$ | | | | | | | $\rho = 0.9$ | | | | | | | $\rho = 0.95$ | | | | | | |
| 0.2 | 0.6 | 3 | 27 | 1.20 | 2.404 | 1.383 | 1.340 | 4.15 | 4 | 15 | 1.37 | 2.579 | 1.097 | 1.080 | 1.76 | 4 | 10 | 1.99 | 2.782 | 0.674 | 0.670 | 1.16 |
| 0.5 | 1 | 5 | 8 | 2.98 | 2.874 | 0.431 | 0.429 | 1.12 | 5 | 8 | 2.98 | 2.874 | 0.431 | 0.429 | 1.00 | 4 | 8 | 3.97 | 2.911 | 0.319 | 0.317 | 1.00 |
| 1 | 1.5 | 4 | 8 | 3.97 | 2.911 | 0.319 | 0.317 | 1.00 | 6 | 8 | 1.99 | 2.782 | 0.674 | 0.670 | 1.00 | 6 | 8 | 1.99 | 2.782 | 0.674 | 0.670 | 1.00 |
| 1.5 | 2 | 6 | 8 | 1.99 | 2.782 | 0.674 | 0.670 | 1.00 | 6 | 8 | 1.99 | 2.782 | 0.674 | 0.670 | 1.00 | 6 | 8 | 1.99 | 2.782 | 0.674 | 0.670 | 1.00 |

Table 4. Optimal parameters and $EATS_1$ values of the VP-AI chart, for $t_s = 0.1$, $EATS_0 = 370$, $n_0 \in \{5, 7\}$, $\rho \in \{0, 0.25, 0.5, 0.75, 0.9, 0.95\}$ and

$(\delta_{\min}, \delta_{\max}) \in \{(0.2, 0.6), (0.5, 1), (1, 1.5), (1.5, 2)\}$

| | | $n_0 = 5$ | | | | | | | | | | | | | | | | | | | |
|---|---|---|---|---|---|---|---|---|---|---|---|---|---|---|---|---|---|---|---|---|---|
| | | $n_S$ | $n_L$ | $t_L$ | $K_2$ | $W_1$ | $W_2$ | $EATS_1$ | $n_S$ | $n_L$ | $t_L$ | $K_2$ | $W_1$ | $W_2$ | $EATS_1$ | $n_S$ | $n_L$ | $t_L$ | $K_2$ | $W_1$ | $W_2$ | $EATS_1$ |
| $\delta_{\min}$ | $\delta_{\max}$ | $\rho = 0$ | | | | | | | $\rho = 0.25$ | | | | | | | $\rho = 0.5$ | | | | | | |
| 0.2 | 0.6 | 2 | 31 | 1.11 | 2.225 | 1.628 | 1.527 | 15.50 | 2 | 31 | 1.11 | 2.225 | 1.628 | 1.527 | 14.38 | 2 | 31 | 1.11 | 2.225 | 1.628 | 1.527 | 11.12 |
| 0.5 | 1 | 2 | 14 | 1.30 | 2.549 | 1.150 | 1.131 | 2.90 | 2 | 13 | 1.34 | 2.579 | 1.096 | 1.080 | 2.71 | 3 | 12 | 1.26 | 2.507 | 1.221 | 1.196 | 2.18 |
| 1 | 1.5 | 3 | 6 | 2.80 | 2.874 | 0.431 | 0.429 | 1.21 | 3 | 6 | 2.80 | 2.874 | 0.431 | 0.429 | 1.18 | 3 | 6 | 2.80 | 2.874 | 0.431 | 0.429 | 1.11 |
| 1.5 | 2 | 3 | 6 | 2.80 | 2.874 | 0.431 | 0.429 | 1.06 | 2 | 6 | 3.70 | 2.911 | 0.319 | 0.317 | 1.05 | 2 | 6 | 3.70 | 2.911 | 0.319 | 0.317 | 1.04 |
| $\delta_{\min}$ | $\delta_{\max}$ | $\rho = 0.75$ | | | | | | | $\rho = 0.9$ | | | | | | | $\rho = 0.95$ | | | | | | |
| 0.2 | 0.6 | 2 | 24 | 1.14 | 2.330 | 1.489 | 1.427 | 6.14 | 2 | 14 | 1.30 | 2.549 | 1.150 | 1.131 | 2.54 | 3 | 9 | 1.45 | 2.648 | 0.967 | 0.957 | 1.47 |
| 0.5 | 1 | 3 | 8 | 1.60 | 2.709 | 0.842 | 0.834 | 1.42 | 3 | 6 | 2.80 | 2.874 | 0.431 | 0.429 | 1.08 | 2 | 6 | 3.70 | 2.911 | 0.319 | 0.317 | 1.04 |
| 1 | 1.5 | 2 | 6 | 3.70 | 2.911 | 0.319 | 0.317 | 1.05 | 2 | 6 | 3.70 | 2.911 | 0.319 | 0.317 | 1.03 | 4 | 6 | 1.90 | 2.782 | 0.674 | 0.670 | 1.01 |
| 1.5 | 2 | 2 | 6 | 3.70 | 2.911 | 0.319 | 0.317 | 1.03 | 4 | 6 | 1.90 | 2.782 | 0.674 | 0.670 | 1.01 | 4 | 6 | 1.90 | 2.782 | 0.674 | 0.670 | 1.00 |
| | | $n_0 = 7$ | | | | | | | | | | | | | | | | | | | |
| | | $n_S$ | $n_L$ | $t_L$ | $K_2$ | $W_1$ | $W_2$ | $EATS_1$ | $n_S$ | $n_L$ | $t_L$ | $K_2$ | $W_1$ | $W_2$ | $EATS_1$ | $n_S$ | $n_L$ | $t_L$ | $K_2$ | $W_1$ | $W_2$ | $EATS_1$ |
| $\delta_{\min}$ | $\delta_{\max}$ | $\rho = 0$ | | | | | | | $\rho = 0.25$ | | | | | | | $\rho = 0.5$ | | | | | | |
| 0.2 | 0.6 | 2 | 31 | 1.19 | 2.417 | 1.364 | 1.324 | 11.09 | 2 | 31 | 1.19 | 2.417 | 1.364 | 1.324 | 10.22 | 2 | 31 | 1.19 | 2.417 | 1.364 | 1.324 | 7.77 |
| 0.5 | 1 | 4 | 16 | 1.30 | 2.549 | 1.150 | 1.131 | 1.13 | 4 | 15 | 1.34 | 2.579 | 1.097 | 1.080 | 1.95 | 4 | 13 | 1.45 | 2.648 | 0.967 | 0.957 | 1.63 |
| 1 | 1.5 | 4 | 8 | 3.70 | 2.911 | 0.319 | 0.317 | 1.10 | 4 | 8 | 3.70 | 2.911 | 0.319 | 0.317 | 1.09 | 4 | 8 | 3.70 | 2.911 | 0.319 | 0.317 | 1.06 |
| 1.5 | 2 | 3 | 8 | 4.60 | 2.931 | 0.253 | 0.252 | 1.03 | 3 | 8 | 4.60 | 2.931 | 0.253 | 0.252 | 1.03 | 2 | 8 | 5.50 | 2.944 | 0.210 | 0.209 | 1.03 |
| $\delta_{\min}$ | $\delta_{\max}$ | $\rho = 0.75$ | | | | | | | $\rho = 0.9$ | | | | | | | $\rho = 0.95$ | | | | | | |
| 0.2 | 0.6 | 3 | 27 | 1.18 | 2.404 | 1.383 | 1.340 | 4.24 | 4 | 16 | 1.30 | 2.549 | 1.150 | 1.131 | 1.86 | 4 | 11 | 1.68 | 2.732 | 0.792 | 0.785 | 1.25 |
| 0.5 | 1 | 4 | 9 | 2.35 | 2.841 | 0.524 | 0.522 | 1.21 | 3 | 8 | 4.60 | 2.931 | 0.253 | 0.252 | 1.05 | 2 | 8 | 5.50 | 2.944 | 0.210 | 0.209 | 1.03 |
| 1 | 1.5 | 3 | 8 | 4.60 | 2.931 | 0.253 | 0.252 | 1.03 | 6 | 8 | 1.90 | 2.782 | 0.674 | 0.670 | 1.02 | 6 | 8 | 1.90 | 2.782 | 0.674 | 0.670 | 1.01 |
| 1.5 | 2 | 2 | 8 | 5.50 | 2.944 | 0.210 | 0.209 | 1.02 | 6 | 8 | 1.90 | 2.782 | 0.674 | 0.670 | 1.01 | 6 | 8 | 1.90 | 2.782 | 0.674 | 0.670 | 1.01 |

Table 5. Comparison of the $ATS_1$ values of the VP-AI chart with the SH-AI, SYN-AI, EWMA-AI, RS-AI and VSSI-AI charts when $t_s = 0.01$, $ATS_0 = 370$, $n_0 \in \{5, 7\}$,

$\rho \in \{0, 0.25, 0.5, 0.75, 0.9, 0.95\}$ and $\delta \in \{0.2, 0.4, 0.6, 0.8, 1, 1.5, 2\}$

| | | | | | | | | | | | | | | | | | | |
|---|---|---|---|---|---|---|---|---|---|---|---|---|---|---|---|---|---|---|
| | SH-AI | SYN-AI | EWMA-AI | RS-AI | VSSI-AI | VP-AI | SH-AI | SYN-AI | EWMA-AI | RS-AI | VSSI-AI | VP-AI | SH-AI | SYN-AI | EWMA-AI | RS-AI | VSSI-AI | VP-AI |
| | | | | | | | | | $n_0 = 5$ | | | | | | | | | |
| $\delta$ | | | $\rho = 0$ | | | | | | $\rho = 0.25$ | | | | | | $\rho = 0.5$ | | | |
| 0.2 | 177.56 | 148.95 | 30.32 | 57.11 | 135.24 | 55.28 | 171.05 | 142.28 | 29.00 | 53.46 | 127.08 | 51.37 | 148.63 | 119.84 | 24.78 | 42.15 | 99.82 | 39.43 |
| 0.4 | 56.55 | 38.57 | 11.11 | 11.28 | 16.33 | 9.75 | 52.65 | 35.62 | 10.59 | 10.40 | 14.36 | 9.02 | 40.61 | 26.83 | 8.95 | 7.86 | 9.30 | 6.89 |
| 0.6 | 20.55 | 13.40 | 6.03 | 4.15 | 4.12 | 3.64 | 18.77 | 12.29 | 5.74 | 3.84 | 3.78 | 3.37 | 13.61 | 9.14 | 4.84 | 2.94 | 2.84 | 2.60 |
| 0.8 | 8.85 | 6.32 | 3.90 | 2.12 | 2.02 | 1.91 | 8.02 | 5.84 | 3.71 | 1.99 | 1.88 | 1.80 | 5.71 | 4.50 | 3.14 | 1.62 | 1.51 | 1.46 |
| 1 | 4.49 | 3.80 | 2.79 | 1.43 | 1.32 | 1.30 | 4.08 | 3.57 | 2.65 | 1.37 | 1.26 | 1.25 | 2.96 | 2.93 | 2.24 | 1.21 | 1.12 | 1.12 |
| 1.5 | 1.57 | 2.15 | 1.50 | 1.04 | 1.02 | 1.02 | 1.47 | 2.11 | 1.43 | 1.03 | 1.01 | 1.00 | 1.24 | 1.30 | 1.23 | 1.01 | 1.00 | 1.00 |
| 2 | 1.08 | 1.15 | 1.08 | 1.00 | 1.00 | 1.00 | 1.06 | 1.13 | 1.06 | 1.00 | 1.00 | 1.00 | 1.02 | 1.10 | 1.02 | 1.00 | 1.00 | 1.00 |
| $\delta$ | | | $\rho = 0.75$ | | | | | | $\rho = 0.9$ | | | | | | $\rho = 0.95$ | | | |
| 0.2 | 98.10 | 72.75 | 16.80 | 22.60 | 46.39 | 19.74 | 41.26 | 27.30 | 9.04 | 7.99 | 9.54 | 7.00 | 17.09 | 11.25 | 5.46 | 3.55 | 3.47 | 3.11 |
| 0.4 | 20.10 | 13.12 | 5.95 | 4.07 | 4.03 | 3.57 | 5.83 | 4.57 | 3.17 | 1.63 | 1.52 | 1.48 | 2.24 | 2.52 | 1.91 | 1.11 | 1.06 | 1.06 |
| 0.6 | 6.04 | 4.69 | 3.22 | 1.67 | 1.56 | 1.51 | 1.88 | 2.32 | 1.71 | 1.07 | 1.03 | 1.03 | 1.11 | 1.18 | 1.11 | 1.00 | 1.00 | 1.00 |
| 0.8 | 2.60 | 2.72 | 2.09 | 1.16 | 1.09 | 1.09 | 1.16 | 1.23 | 1.15 | 1.00 | 1.00 | 1.00 | 1.00 | 1.09 | 1.00 | 1.00 | 1.00 | 1.00 |
| 1 | 1.54 | 2.14 | 1.48 | 1.03 | 1.02 | 1.02 | 1.02 | 1.10 | 1.02 | 1.00 | 1.00 | 1.00 | 1.00 | 1.08 | 1.00 | 1.00 | 1.00 | 1.00 |
| 1.5 | 1.02 | 1.10 | 1.02 | 1.00 | 1.00 | 1.00 | 1.00 | 1.08 | 1.00 | 1.00 | 1.00 | 1.00 | 1.00 | 1.08 | 1.00 | 1.00 | 1.00 | 1.00 |
| 2 | 1.00 | 1.08 | 1.00 | 1.00 | 1.00 | 1.00 | 1.00 | 1.08 | 1.00 | 1.00 | 1.00 | 1.00 | 1.00 | 1.08 | 1.00 | 1.00 | 1.00 | 1.00 |
| | | | | | | | | | $n_0 = 7$ | | | | | | | | | |
| $\delta$ | | | $\rho = 0$ | | | | | | $\rho = 0.25$ | | | | | | $\rho = 0.5$ | | | |
| 0.2 | 143.79 | 115.11 | 23.94 | 39.94 | 102.84 | 43.42 | 137.44 | 108.97 | 22.85 | 37.17 | 95.61 | 39.98 | 116.18 | 88.98 | 19.47 | 28.77 | 72.37 | 29.67 |
| 0.4 | 38.27 | 25.19 | 8.63 | 7.40 | 10.29 | 6.39 | 35.33 | 23.15 | 8.22 | 6.83 | 9.03 | 5.92 | 26.50 | 17.22 | 6.94 | 5.20 | 5.89 | 4.55 |
| 0.6 | 12.67 | 8.57 | 4.67 | 2.78 | 2.67 | 2.46 | 11.51 | 7.88 | 4.45 | 2.57 | 2.47 | 2.29 | 8.22 | 5.95 | 3.76 | 2.02 | 1.91 | 1.82 |
| 0.8 | 5.30 | 4.26 | 3.02 | 1.55 | 1.44 | 1.40 | 4.81 | 3.98 | 2.88 | 1.48 | 1.36 | 1.34 | 3.46 | 3.21 | 2.44 | 1.28 | 1.17 | 1.17 |
| 1 | 2.76 | 2.81 | 2.16 | 1.18 | 1.10 | 1.10 | 2.53 | 2.68 | 2.06 | 1.15 | 1.07 | 1.07 | 1.92 | 2.34 | 1.73 | 1.07 | 1.03 | 1.03 |
| 1.5 | 1.20 | 1.27 | 1.19 | 1.01 | 1.00 | 1.00 | 1.16 | 1.23 | 1.15 | 1.00 | 1.00 | 1.00 | 1.06 | 1.14 | 1.06 | 1.00 | 1.00 | 1.00 |
| 2 | 1.01 | 1.09 | 1.01 | 1.00 | 1.00 | 1.00 | 1.01 | 1.09 | 1.01 | 1.00 | 1.00 | 1.00 | 1.00 | 1.08 | 1.00 | 1.00 | 1.00 | 1.00 |
| $\delta$ | | | $\rho = 0.75$ | | | | | | $\rho = 0.9$ | | | | | | $\rho = 0.95$ | | | |
| 0.2 | 71.49 | 50.31 | 13.12 | 14.93 | 30.91 | 13.63 | 26.97 | 17.52 | 7.01 | 5.28 | 6.03 | 4.62 | 10.42 | 7.24 | 4.23 | 2.39 | 2.28 | 2.13 |
| 0.4 | 12.38 | 8.40 | 4.61 | 2.72 | 2.62 | 2.42 | 3.52 | 3.25 | 2.46 | 1.29 | 1.18 | 1.18 | 1.53 | 2.14 | 1.47 | 1.03 | 1.01 | 1.01 |
| 0.6 | 3.64 | 3.32 | 2.51 | 1.30 | 1.20 | 1.19 | 1.35 | 1.41 | 1.33 | 1.02 | 1.01 | 1.01 | 1.02 | 1.10 | 1.02 | 1.00 | 1.00 | 1.00 |
| 0.8 | 1.73 | 2.23 | 1.61 | 1.05 | 1.02 | 1.02 | 1.03 | 1.11 | 1.03 | 1.00 | 1.00 | 1.00 | 1.00 | 1.08 | 1.00 | 1.00 | 1.00 | 1.00 |
| 1 | 1.19 | 1.26 | 1.18 | 1.01 | 1.00 | 1.00 | 1.00 | 1.08 | 1.00 | 1.00 | 1.00 | 1.00 | 1.00 | 1.08 | 1.00 | 1.00 | 1.00 | 1.00 |
| 1.5 | 1.00 | 1.08 | 1.00 | 1.00 | 1.00 | 1.00 | 1.00 | 1.08 | 1.00 | 1.00 | 1.00 | 1.00 | 1.00 | 1.08 | 1.00 | 1.00 | 1.00 | 1.00 |
| 2 | 1.00 | 1.08 | 1.00 | 1.00 | 1.00 | 1.00 | 1.00 | 1.08 | 1.00 | 1.00 | 1.00 | 1.00 | 1.00 | 1.08 | 1.00 | 1.00 | 1.00 | 1.00 |

Table 6. Comparison of the $SDTS_1$ values of the VP-AI chart with the SH-AI, SYN-AI, EWMA-AI, RS-AI and VSSI-AI charts when $t_s$ = 0.01, $ATS_0$ = 370, $n_0 \in \{5, 7\}$, $\rho \in \{0, 0.25, 0.5, 0.75, 0.9, 0.95\}$ and $\delta \in \{0.2, 0.4, 0.6, 0.8, 1, 1.5, 2\}$

| | SH-AI | SYN-AI | EWMA-AI | RS-AI | VSSI-AI | VP-AI | SH-AI | SYN-AI | EWMA-AI | RS-AI | VSSI-AI | VP-AI | SH-AI | SYN-AI | EWMA-AI | RS-AI | VSSI-AI | VP-AI |
|---|---|---|---|---|---|---|---|---|---|---|---|---|---|---|---|---|---|---|
| | | | | | | | | | | $n_0 = 5$ | | | | | | | | |
| $\delta$ | $\rho = 0$ | | | | | | $\rho = 0.25$ | | | | | | $\rho = 0.5$ | | | | | |
| 0.2 | 177.23 | 147.15 | 19.18 | 56.53 | 135.39 | 55.63 | 170.71 | 140.33 | 18.88 | 52.90 | 127.25 | 51.72 | 148.27 | 117.58 | 15.30 | 41.69 | 100.05 | 39.76 |
| 0.4 | 56.09 | 36.08 | 6.33 | 10.96 | 16.69 | 9.89 | 52.19 | 33.12 | 6.06 | 10.07 | 14.72 | 9.17 | 40.14 | 24.53 | 5.00 | 7.51 | 9.64 | 7.01 |
| 0.6 | 20.06 | 11.49 | 3.22 | 4.16 | 4.14 | 3.74 | 18.28 | 10.39 | 3.05 | 3.82 | 3.80 | 3.48 | 13.11 | 7.38 | 2.52 | 2.90 | 2.88 | 2.72 |
| 0.8 | 8.34 | 4.72 | 1.98 | 2.03 | 2.15 | 2.13 | 7.51 | 4.25 | 1.86 | 1.88 | 2.07 | 1.75 | 5.19 | 3.03 | 1.55 | 1.55 | 1.49 | 1.62 |
| 1 | 3.96 | 2.33 | 1.37 | 1.48 | 1.44 | 1.43 | 3.55 | 2.09 | 1.30 | 1.37 | 1.76 | 1.76 | 2.41 | 1.52 | 1.09 | 1.08 | 1.59 | 1.59 |
| 1.5 | 0.94 | 0.62 | 0.72 | 0.69 | 1.01 | 1.02 | 0.84 | 0.56 | 0.68 | 0.63 | 1.01 | 1.01 | 0.54 | 0.60 | 0.50 | 0.48 | 1.00 | 1.00 |
| 2 | 0.29 | 0.30 | 0.28 | 0.27 | 0.99 | 1.41 | 0.24 | 0.30 | 0.24 | 0.24 | 0.99 | 1.41 | 0.13 | 0.20 | 0.50 | 0.13 | 0.99 | 1.41 |
| $\delta$ | $\rho = 0.75$ | | | | | | $\rho = 0.9$ | | | | | | $\rho = 0.95$ | | | | | |
| 0.2 | 97.69 | 70.07 | 10.06 | 22.26 | 46.73 | 19.99 | 40.79 | 24.99 | 5.07 | 7.64 | 9.88 | 7.12 | 16.59 | 9.47 | 2.87 | 3.51 | 3.51 | 3.24 |
| 0.4 | 19.61 | 11.21 | 3.16 | 4.08 | 4.05 | 3.67 | 5.31 | 3.09 | 1.56 | 1.57 | 1.51 | 1.64 | 1.67 | 1.07 | 0.95 | 0.94 | 1.50 | 1.51 |
| 0.6 | 5.52 | 3.21 | 1.60 | 1.61 | 1.55 | 1.51 | 1.29 | 0.83 | 0.85 | 0.86 | 1.04 | 1.04 | 0.35 | 0.40 | 0.34 | 0.33 | 0.99 | 1.41 |
| 0.8 | 2.05 | 1.30 | 1.03 | 1.08 | 1.54 | 1.55 | 0.42 | 0.50 | 0.40 | 0.39 | 0.99 | 1.41 | 0.06 | 0.20 | 0.06 | 0.06 | 0.99 | 1.72 |
| 1 | 0.91 | 0.60 | 0.71 | 0.67 | 1.01 | 1.02 | 0.13 | 0.20 | 0.13 | 0.13 | 0.99 | 1.41 | 0.00 | 0.20 | 0.00 | 0.00 | 0.99 | 0.99 |
| 1.5 | 0.14 | 0.20 | 0.14 | 0.14 | 0.99 | 1.41 | 0.00 | 0.20 | 0.00 | 0.00 | 0.99 | 0.99 | 0.00 | 0.20 | 0.00 | 0.00 | 0.99 | 0.99 |
| 2 | 0.01 | 0.20 | 0.01 | 0.01 | 0.99 | 0.99 | 0.00 | 0.20 | 0.00 | 0.00 | 0.99 | 0.99 | 0.00 | 0.20 | 0.00 | 0.00 | 0.99 | 0.21 |
| | | | | | | | | | | $n_0 = 7$ | | | | | | | | |
| $\delta$ | $\rho = 0$ | | | | | | $\rho = 0.25$ | | | | | | $\rho = 0.5$ | | | | | |
| 0.2 | 143.42 | 112.76 | 15.19 | 39.51 | 103.19 | 43.85 | 137.07 | 106.51 | 14.27 | 36.75 | 95.98 | 40.41 | 115.78 | 86.35 | 11.90 | 28.40 | 72.79 | 30.08 |
| 0.4 | 37.79 | 22.88 | 4.75 | 7.04 | 10.78 | 6.62 | 34.85 | 20.96 | 4.52 | 6.47 | 9.52 | 6.15 | 26.01 | 15.16 | 3.75 | 4.86 | 6.35 | 4.78 |
| 0.6 | 12.16 | 6.83 | 2.39 | 2.73 | 2.70 | 2.55 | 11.00 | 6.26 | 2.28 | 2.51 | 2.50 | 2.40 | 7.71 | 4.36 | 1.90 | 1.91 | 2.04 | 2.03 |
| 0.8 | 4.78 | 2.79 | 1.48 | 1.67 | 1.59 | 1.57 | 4.28 | 2.51 | 1.41 | 1.55 | 1.50 | 1.70 | 2.92 | 1.74 | 1.19 | 1.21 | 1.98 | 1.98 |
| 1 | 2.21 | 1.40 | 1.07 | 1.03 | 1.53 | 1.54 | 1.97 | 1.25 | 1.01 | 1.05 | 1.50 | 1.51 | 1.32 | 0.85 | 0.86 | 0.87 | 1.45 | 1.45 |
| 1.5 | 0.49 | 0.50 | 0.46 | 0.44 | 1.41 | 1.41 | 0.43 | 0.50 | 0.41 | 0.40 | 1.40 | 1.41 | 0.25 | 0.30 | 0.25 | 0.25 | 1.40 | 1.72 |
| 2 | 0.11 | 0.20 | 0.11 | 0.11 | 1.40 | 1.99 | 0.08 | 0.20 | 0.08 | 0.08 | 1.40 | 0.99 | 0.03 | 0.20 | 0.03 | 0.03 | 1.40 | 1.99 |
| $\delta$ | $\rho = 0.75$ | | | | | | $\rho = 0.9$ | | | | | | $\rho = 0.95$ | | | | | |
| 0.2 | 71.05 | 47.71 | 7.59 | 14.61 | 31.41 | 13.98 | 26.48 | 15.46 | 3.81 | 4.95 | 6.49 | 4.86 | 9.92 | 5.63 | 2.15 | 2.32 | 2.33 | 2.27 |
| 0.4 | 11.87 | 6.77 | 2.38 | 2.67 | 2.64 | 2.54 | 2.98 | 1.77 | 1.20 | 1.23 | 1.99 | 1.99 | 0.91 | 0.60 | 0.71 | 0.67 | 1.42 | 1.43 |
| 0.6 | 3.11 | 1.84 | 1.23 | 1.26 | 2.01 | 2.01 | 0.69 | 0.70 | 0.60 | 0.59 | 1.41 | 1.42 | 0.14 | 0.20 | 0.14 | 0.14 | 1.40 | 1.72 |
| 0.8 | 1.12 | 0.73 | 0.80 | 0.78 | 1.43 | 1.44 | 0.18 | 0.30 | 0.18 | 0.18 | 1.40 | 1.72 | 0.01 | 0.20 | 0.00 | 0.01 | 1.40 | 1.99 |
| 1 | 0.47 | 0.50 | 0.45 | 0.43 | 1.40 | 1.41 | 0.03 | 0.20 | 0.18 | 0.03 | 1.40 | 1.99 | 0.00 | 0.20 | 0.00 | 0.00 | 0.81 | 0.99 |
| 1.5 | 0.04 | 0.20 | 0.04 | 0.04 | 1.40 | 1.99 | 0.00 | 0.20 | 0.00 | 0.00 | 0.77 | 0.99 | 0.00 | 0.20 | 0.00 | 0.00 | 2.21 | 0.21 |
| 2 | 0.00 | 0.20 | 0.00 | 0.00 | 0.81 | 0.99 | 0.00 | 0.20 | 0.00 | 0.00 | 0.21 | 0.21 | 0.00 | 0.20 | 0.00 | 0.00 | 2.21 | 0.38 |

Table 7. Comparison of the $EATS_1$ values of the VP-AI chart with the SH-AI, SYN-AI, EWMA-AI, RS-AI and VSSI-AI charts when $t_S = 0.01$, $EATS_0 = 370$, $n_0 \in \{5, 7\}$, $\rho \in \{0, 0.25, 0.5, 0.75, 0.9, 0.95\}$ and $(\delta_{min}, \delta_{max}) \in \{(0.2, 0.6), (0.5, 1), (1, 1.5), (1.5, 2)\}$

| | | SH-AI | SYN-AI | EWMA-AI | RS-AI | VSSI-AI | VP-AI | SH-AI | SYN-AI | EWMA-AI | RS-AI | VSSI-AI | VP-AI |
|---|---|---|---|---|---|---|---|---|---|---|---|---|---|
| | | | | | | | $n_0 = 5$ | | | | | | |
| $\delta_{min}$ | $\delta_{max}$ | | | $\rho = 0$ | | | | | | $\rho = 0.25$ | | | |
| 0.2 | 0.6 | 70.20 | 52.19 | 13.56 | 16.72 | 32.55 | 15.40 | 66.14 | 48.84 | 12.93 | 15.50 | 29.63 | 14.28 |
| 0.5 | 1.0 | 13.29 | 9.11 | 4.71 | 2.95 | 3.13 | 2.78 | 12.12 | 8.39 | 4.49 | 2.74 | 2.89 | 2.59 |
| 1.0 | 1.5 | 2.59 | 2.72 | 2.06 | 1.16 | 1.10 | 1.10 | 2.38 | 2.61 | 1.96 | 1.14 | 1.08 | 1.08 |
| 1.5 | 2.0 | 1.25 | 1.32 | 1.24 | 1.01 | 1.01 | 1.01 | 1.20 | 1.27 | 1.20 | 1.01 | 1.00 | 1.00 |
| $\delta_{min}$ | $\delta_{max}$ | | | $\rho = 0.5$ | | | | | | $\rho = 0.75$ | | | |
| 0.2 | 0.6 | 53.27 | 38.46 | 10.99 | 11.90 | 21.12 | 11.04 | 29.57 | 20.53 | 7.38 | 6.25 | 8.90 | 6.05 |
| 0.5 | 1.0 | 8.77 | 6.35 | 3.80 | 2.15 | 2.22 | 2.06 | 3.98 | 3.52 | 2.54 | 1.37 | 1.34 | 1.31 |
| 1.0 | 1.5 | 1.82 | 2.30 | 1.65 | 1.07 | 1.04 | 1.04 | 1.17 | 1.24 | 1.17 | 1.01 | 1.00 | 1.00 |
| 1.5 | 2.0 | 1.09 | 1.08 | 1.09 | 1.00 | 1.00 | 1.00 | 1.00 | 1.09 | 1.00 | 1.00 | 1.00 | 1.00 |
| $\delta_{min}$ | $\delta_{max}$ | | | $\rho = 0.9$ | | | | | | $\rho = 0.95$ | | | |
| 0.2 | 0.6 | 10.09 | 7.28 | 2.43 | 2.45 | 2.76 | 2.43 | 3.97 | 3.55 | 2.43 | 1.40 | 1.42 | 1.37 |
| 0.5 | 1.0 | 1.47 | 2.13 | 1.39 | 1.04 | 1.02 | 1.02 | 1.06 | 1.14 | 1.06 | 1.00 | 1.00 | 1.00 |
| 1.0 | 1.5 | 1.00 | 1.08 | 1.26 | 1.00 | 1.00 | 1.00 | 1.00 | 1.08 | 1.00 | 1.00 | 1.00 | 1.00 |
| 1.5 | 2.0 | 1.00 | 1.08 | 1.00 | 1.00 | 1.00 | 1.00 | 1.00 | 1.08 | 1.00 | 1.00 | 1.00 | 1.00 |
| | | | | | | | $n_0 = 7$ | | | | | | |
| $\delta_{min}$ | $\delta_{max}$ | | | $\rho = 0$ | | | | | | $\rho = 0.25$ | | | |
| 0.2 | 0.6 | 50.70 | 36.44 | 10.60 | 11.23 | 22.54 | 10.95 | 47.44 | 33.89 | 10.11 | 10.39 | 20.39 | 10.09 |
| 0.5 | 1.0 | 8.16 | 5.98 | 3.66 | 2.05 | 2.10 | 1.95 | 7.42 | 5.54 | 3.49 | 1.92 | 1.96 | 1.83 |
| 1.0 | 1.5 | 1.73 | 2.25 | 1.59 | 1.06 | 1.03 | 1.04 | 1.62 | 2.19 | 1.52 | 1.05 | 1.02 | 1.02 |
| 1.5 | 2.0 | 1.07 | 1.15 | 1.07 | 1.00 | 1.00 | 1.00 | 1.05 | 1.13 | 1.05 | 1.00 | 1.00 | 1.00 |
| $\delta_{min}$ | $\delta_{max}$ | | | $\rho = 0.5$ | | | | | | $\rho = 0.75$ | | | |
| 0.2 | 0.6 | 37.29 | 26.18 | 8.57 | 7.96 | 14.24 | 7.67 | 19.58 | 13.52 | 5.74 | 4.22 | 5.87 | 4.15 |
| 0.5 | 1.0 | 5.34 | 4.32 | 2.96 | 1.58 | 1.57 | 1.51 | 2.51 | 2.69 | 1.98 | 1.16 | 1.12 | 1.12 |
| 1.0 | 1.5 | 1.33 | 1.40 | 1.30 | 1.02 | 1.01 | 1.01 | 1.05 | 1.12 | 1.05 | 1.00 | 1.00 | 1.00 |
| 1.5 | 2.0 | 1.02 | 1.16 | 1.02 | 1.00 | 1.00 | 1.00 | 1.00 | 1.08 | 1.00 | 1.00 | 1.00 | 1.00 |
| $\delta_{min}$ | $\delta_{max}$ | | | $\rho = 0.9$ | | | | | | $\rho = 0.95$ | | | |
| 0.2 | 0.6 | 6.30 | 4.93 | 3.10 | 1.78 | 1.90 | 1.76 | 2.56 | 2.74 | 1.90 | 1.19 | 1.17 | 1.16 |
| 0.5 | 1.0 | 1.18 | 1.25 | 1.17 | 1.01 | 1.00 | 1.00 | 1.01 | 1.09 | 1.01 | 1.00 | 1.00 | 1.00 |
| 1.0 | 1.5 | 1.00 | 1.08 | 1.00 | 1.00 | 1.00 | 1.00 | 1.00 | 1.08 | 1.00 | 1.00 | 1.00 | 1.00 |
| 1.5 | 2.0 | 1.00 | 1.08 | 1.00 | 1.00 | 1.00 | 1.00 | 1.00 | 1.08 | 1.00 | 1.00 | 1.00 | 1.00 |

Table 8. $ATS_1$ values of the EWMA-AI and VP-AI charts due to misspecification of the value of the correlation coefficient ($\rho_{miss}$), where $\rho_{miss} \in \{0.3, 0.7\}$, $t_s = 0.01$, $ATS_0 = 370$, $n_0 \in \{5, 7\}$, $\rho \in \{0.25, 0.5, 0.75, 0.9, 0.95\}$ and $\delta \in \{0.2, 0.4, 0.6, 0.8, 1, 1.5, 2\}$

| | | $\rho = 0.25$ | | $\rho = 0.5$ | | $\rho = 0.75$ | | $\rho = 0.9$ | | $\rho = 0.95$ | |
|---|---|---|---|---|---|---|---|---|---|---|---|
| $\rho_{miss}$ | $\delta$ | EWMA-AI | VP-AI | EWMA-AI | VP-AI | EWMA-AI | VP-AI | EWMA-AI | VP-AI | EWMA-AI | VP-AI |
| | | | | | | $n_0 = 5$ | | | | | |
| 0.3 | 0.2 | 28.40 | 49.59 | 28.40 | 49.59 | 25.32 | 49.59 | 35.25 | 57.11 | 45.10 | 83.95 |
| | 0.4 | 10.35 | 8.69 | 10.39 | 8.84 | 9.24 | 10.64 | 14.52 | 22.36 | 24.10 | 26.75 |
| | 0.6 | 5.61 | 3.24 | 5.64 | 3.28 | 5.04 | 4.18 | 9.69 | 5.86 | 15.95 | 5.72 |
| | 0.8 | 3.63 | 1.74 | 3.65 | 1.79 | 3.34 | 1.93 | 6.58 | 1.93 | 7.49 | 1.94 |
| | 1 | 2.60 | 1.22 | 2.61 | 1.22 | 2.41 | 1.25 | 3.84 | 1.22 | 3.84 | 1.25 |
| | 1.5 | 1.40 | 1.02 | 1.40 | 1.02 | 1.23 | 1.02 | 1.43 | 1.02 | 1.41 | 1.02 |
| | 2 | 1.05 | 1.00 | 1.05 | 1.00 | 1.02 | 1.01 | 1.05 | 1.01 | 1.35 | 1.01 |
| 0.7 | 0.2 | 19.06 | 24.11 | 19.06 | 24.11 | 18.82 | 24.11 | 20.66 | 27.33 | 25.08 | 42.04 |
| | 0.4 | 6.87 | 4.90 | 6.77 | 4.53 | 6.70 | 4.32 | 7.70 | 7.54 | 11.48 | 9.22 |
| | 0.6 | 3.74 | 1.99 | 3.67 | 1.87 | 3.63 | 1.74 | 4.61 | 2.00 | 6.83 | 1.92 |
| | 0.8 | 2.45 | 1.22 | 2.40 | 1.16 | 2.36 | 1.14 | 2.92 | 1.14 | 3.17 | 1.16 |
| | 1 | 1.77 | 1.03 | 1.72 | 1.03 | 1.67 | 1.03 | 1.80 | 1.03 | 1.80 | 1.03 |
| | 1.5 | 1.05 | 1.01 | 1.05 | 1.01 | 1.05 | 1.00 | 1.05 | 1.01 | 1.05 | 1.01 |
| | 2 | 1.00 | 1.00 | 1.00 | 1.00 | 1.00 | 1.00 | 1.00 | 1.00 | 1.07 | 1.00 |
| | | | | | | $n_0 = 7$ | | | | | |
| 0.3 | 0.2 | 22.37 | 38.43 | 22.45 | 38.43 | 23.28 | 38.43 | 28.39 | 45.95 | 37.27 | 70.11 |
| | 0.4 | 8.04 | 5.71 | 8.07 | 5.81 | 8.57 | 7.65 | 11.76 | 15.85 | 22.13 | 15.81 |
| | 0.6 | 4.35 | 2.21 | 4.37 | 2.27 | 4.77 | 3.08 | 8.05 | 3.09 | 10.75 | 3.08 |
| | 0.8 | 2.82 | 1.31 | 2.84 | 1.33 | 3.26 | 1.34 | 4.43 | 1.33 | 4.51 | 1.34 |
| | 1 | 2.01 | 1.07 | 2.03 | 1.07 | 2.25 | 1.07 | 2.41 | 1.08 | 2.41 | 1.08 |
| | 1.5 | 1.14 | 1.01 | 1.14 | 1.01 | 1.14 | 1.01 | 1.14 | 1.01 | 1.31 | 1.01 |
| | 2 | 1.01 | 1.00 | 1.01 | 1.00 | 1.01 | 1.00 | 1.03 | 1.00 | 1.43 | 1.00 |
| 0.7 | 0.2 | 15.01 | 17.05 | 14.82 | 17.05 | 14.71 | 17.05 | 16.27 | 20.18 | 20.09 | 32.65 |
| | 0.4 | 5.36 | 3.42 | 5.25 | 3.13 | 5.20 | 2.92 | 6.07 | 4.94 | 10.05 | 4.95 |
| | 0.6 | 2.92 | 1.48 | 2.86 | 1.38 | 2.82 | 1.33 | 3.64 | 1.33 | 4.49 | 1.33 |
| | 0.8 | 1.92 | 1.06 | 1.86 | 1.04 | 1.83 | 1.04 | 2.02 | 1.04 | 2.04 | 1.05 |
| | 1 | 1.37 | 1.01 | 1.32 | 1.01 | 1.30 | 1.01 | 1.31 | 1.02 | 1.31 | 1.01 |
| | 1.5 | 1.01 | 1.00 | 1.01 | 1.00 | 1.01 | 1.00 | 1.01 | 1.00 | 1.05 | 1.00 |
| | 2 | 1.00 | 1.00 | 1.00 | 1.00 | 1.00 | 1.00 | 1.00 | 1.00 | 1.11 | 1.00 |

Table 9. $ATS_1$ values of the EWMA-AI and VP-AI charts for bivariate $t$ distribution with $\nu \in \{3, 10, 20\}$ degrees of freedom when $\rho \in \{0.25, 0.5, 0.75, 0.9, 0.95\}$ and $\delta \in \{0, 0.2, 0.4, 0.6, 0.8, 1, 1.5, 2\}$

| | | $\rho = 0.25$ | | $\rho = 0.5$ | | $\rho = 0.75$ | | $\rho = 0.9$ | | $\rho = 0.95$ | |
|---|---|---|---|---|---|---|---|---|---|---|---|
| $\nu$ | $\delta$ | EWMA-AI | VP-AI | EWMA-AI | VP-AI | EWMA-AI | VP-AI | EWMA-AI | VP-AI | EWMA-AI | VP-AI |
| 3 | 0 | 214.63 | 284.09 | 215.65 | 287.46 | 212.72 | 288.06 | 214.03 | 286.52 | 211.56 | 284.78 |
| | 0.2 | 49.31 | 113.82 | 39.66 | 90.13 | 22.77 | 45.25 | 9.64 | 9.83 | 5.51 | 3.47 |
| | 0.4 | 11.87 | 14.59 | 9.55 | 9.39 | 6.02 | 4.00 | 3.37 | 1.86 | 2.34 | 1.28 |
| | 0.6 | 5.77 | 3.80 | 4.90 | 2.92 | 3.42 | 1.92 | 2.17 | 1.21 | 1.63 | 1.21 |
| | 0.8 | 3.87 | 2.17 | 3.35 | 1.86 | 2.47 | 1.35 | 1.69 | 1.07 | 1.24 | 1.02 |
| | 1 | 2.95 | 1.61 | 2.61 | 1.42 | 2.00 | 1.15 | 1.38 | 1.03 | 1.05 | 1.01 |
| | 1.5 | 1.96 | 1.13 | 1.78 | 1.08 | 1.40 | 1.03 | 1.03 | 1.01 | 1.00 | 0.99 |
| | 2 | 1.54 | 1.04 | 1.38 | 1.03 | 1.09 | 1.01 | 1.00 | 1.00 | 1.00 | 1.00 |
| 10 | 0 | 341.56 | 367.99 | 343.26 | 365.01 | 337.59 | 372.63 | 338.56 | 368.68 | 339.21 | 366.87 |
| | 0.2 | 43.23 | 79.91 | 34.54 | 61.43 | 20.18 | 29.90 | 9.30 | 7.81 | 5.48 | 3.16 |
| | 0.4 | 11.20 | 11.06 | 9.14 | 7.63 | 5.96 | 3.65 | 3.40 | 1.94 | 2.36 | 1.39 |
| | 0.6 | 5.74 | 3.43 | 4.87 | 2.76 | 3.45 | 1.92 | 2.19 | 1.29 | 1.62 | 1.08 |
| | 0.8 | 3.89 | 2.13 | 3.38 | 1.89 | 2.49 | 1.46 | 1.69 | 1.10 | 1.26 | 1.02 |
| | 1 | 2.95 | 1.70 | 2.60 | 1.51 | 2.00 | 1.22 | 1.39 | 1.03 | 1.06 | 1.01 |
| | 1.5 | 1.97 | 1.20 | 1.77 | 1.14 | 1.41 | 1.04 | 1.03 | 1.01 | 1.00 | 1.00 |
| | 2 | 1.52 | 1.05 | 1.39 | 1.04 | 1.10 | 1.01 | 1.00 | 1.00 | 1.00 | 1.00 |
| 20 | 0 | 356.94 | 371.32 | 356.68 | 369.52 | 354.70 | 371.48 | 358.40 | 367.99 | 360.90 | 368.82 |
| | 0.2 | 42.73 | 77.29 | 34.31 | 60.08 | 20.37 | 29.45 | 9.29 | 7.73 | 5.50 | 3.19 |
| | 0.4 | 11.17 | 10.88 | 9.22 | 7.57 | 5.93 | 3.61 | 3.39 | 1.92 | 2.35 | 1.39 |
| | 0.6 | 5.77 | 3.48 | 4.89 | 2.73 | 3.45 | 1.94 | 2.20 | 1.32 | 1.64 | 1.09 |
| | 0.8 | 3.87 | 2.17 | 3.37 | 1.89 | 2.50 | 1.47 | 1.69 | 1.10 | 1.27 | 1.02 |
| | 1 | 2.96 | 1.69 | 2.61 | 1.53 | 2.00 | 1.23 | 1.40 | 1.03 | 1.06 | 1.01 |
| | 1.5 | 1.95 | 1.21 | 1.77 | 1.14 | 1.41 | 1.03 | 1.03 | 1.01 | 1.00 | 1.00 |
| | 2 | 1.53 | 1.05 | 1.38 | 1.03 | 1.10 | 1.01 | 1.00 | 1.00 | 1.00 | 1.00 |

Table 10. $ATS_1$ values of the EWMA-AI and VP-AI charts for bivariate gamma, $G(\beta, \alpha)$ distribution, with $\beta \in \{1, 2\}$ and $\alpha = 1$ when $\rho \in \{0.25, 0.5, 0.75, 0.9, 0.95\}$ and $\delta \in \{0, 0.2, 0.4, 0.6, 0.8, 1, 1.5, 2\}$

| | | $\rho = 0.25$ | | $\rho = 0.5$ | | $\rho = 0.75$ | | $\rho = 0.9$ | | $\rho = 0.95$ | |
|---|---|---|---|---|---|---|---|---|---|---|---|
| | $\delta$ | EWMA-AI | VP-AI | EWMA-AI | VP-AI | EWMA-AI | VP-AI | EWMA-AI | VP-AI | EWMA-AI | VP-AI |
| $G(1, 1)$ | 0 | 249.40 | 393.10 | 200.90 | 285.90 | 128.61 | 177.64 | 81.43 | 112.42 | 66.18 | 97.06 |
| | 0.2 | 37.28 | 90.25 | 29.99 | 65.12 | 19.27 | 35.28 | 9.97 | 12.94 | 5.63 | 6.24 |
| | 0.4 | 11.55 | 15.75 | 9.55 | 11.11 | 6.23 | 5.19 | 3.44 | 2.45 | 2.34 | 1.11 |
| | 0.6 | 5.97 | 4.43 | 5.08 | 3.56 | 3.50 | 2.53 | 2.20 | 1.10 | 1.68 | 1.04 |
| | 0.8 | 3.98 | 2.71 | 3.44 | 2.41 | 2.52 | 1.38 | 1.73 | 1.05 | 1.26 | 1.01 |
| | 1 | 3.00 | 2.02 | 2.64 | 1.74 | 2.02 | 1.11 | 1.43 | 1.03 | 1.07 | 1.01 |
| | 1.5 | 1.96 | 1.15 | 1.79 | 1.07 | 1.44 | 1.03 | 1.04 | 1.01 | 1.00 | 1.00 |
| | 2 | 1.55 | 1.01 | 1.41 | 1.01 | 1.11 | 1.01 | 1.00 | 1.00 | 1.00 | 1.00 |
| $G(2, 1)$ | 0 | 44.09 | 31.73 | 31.36 | 32.53 | 30.92 | 30.10 | 26.48 | 30.74 | 26.16 | 34.86 |
| | 0.2 | 21.02 | 23.24 | 18.21 | 20.72 | 13.42 | 15.43 | 8.48 | 9.43 | 5.48 | 5.43 |
| | 0.4 | 9.63 | 10.29 | 8.40 | 8.07 | 5.97 | 5.01 | 3.46 | 2.53 | 2.38 | 1.15 |
| | 0.6 | 5.78 | 4.74 | 5.03 | 3.79 | 3.58 | 2.57 | 2.27 | 1.15 | 1.70 | 1.05 |
| | 0.8 | 4.04 | 2.82 | 3.53 | 2.49 | 2.59 | 1.67 | 1.76 | 1.06 | 1.34 | 1.03 |
| | 1 | 3.12 | 2.16 | 2.74 | 1.95 | 2.08 | 1.17 | 1.48 | 1.05 | 1.14 | 1.02 |
| | 1.5 | 2.03 | 1.41 | 1.84 | 1.14 | 1.49 | 1.05 | 1.10 | 1.02 | 1.02 | 1.01 |
| | 2 | 1.59 | 1.05 | 1.46 | 1.03 | 1.20 | 1.01 | 1.02 | 1.01 | 1.00 | 1.00 |

Table 11. Implementation of the VP-AI chart using the dataset on a spring manufacturing process

| Sample no., $r$ | $X_1$ | $X_2$ | $X_3$ | $X_4$ | $X_5$ | $X_6$ | $M_1$ | $M_2$ | $M_3$ | $M_4$ | $M_5$ | $M_6$ | $\bar{X}_r$ | $\bar{M}_r$ | $Y^*_{X_r}$ | $Z_r$ | $t_S$ or $t_L$ (hours) | Total time elapsed (hours) |
|---|---|---|---|---|---|---|---|---|---|---|---|---|---|---|---|---|---|---|
| 1 | 46.32 | 45.79 | 45.88 | | | | 28.14 | 28.31 | 28.27 | | | | 46.00 | 28.24 | 45.93 | 1.0908 ∈ $I_2$ | 2.8 | 2.8 |
| 2 | 45.88 | 45.80 | 45.85 | 45.91 | 45.80 | 45.91 | 28.20 | 28.26 | 28.50 | 28.35 | 28.30 | 28.32 | 45.86 | 28.32 | 45.90 | 0.9505 ∈ $I_2$ | 0.1 | 2.9 |
| 3 | 45.93 | 45.83 | 45.75 | 45.75 | 45.52 | 45.58 | 28.20 | 28.29 | 28.30 | 28.29 | 28.38 | 28.29 | 45.73 | 28.29 | 45.73 | -2.3068 ∈ $I_2$ | 0.1 | 3 |
| 4 | 45.81 | 45.99 | 45.78 | 46.02 | 45.85 | 45.77 | 28.22 | 28.26 | 28.27 | 28.27 | 28.28 | 28.30 | 45.87 | 28.27 | 45.84 | -0.2026 ∈ $I_1$ | 0.1 | 3.1 |
| 5 | 45.94 | 46.04 | 45.77 | | | | 28.36 | 28.27 | 28.32 | | | | 45.92 | 28.32 | 45.95 | 1.3691 ∈ $I_2$ | 2.8 | 5.9 |
| 6 | 45.67 | 45.77 | 45.93 | 45.77 | 45.92 | 46.04 | 28.30 | 28.34 | 28.29 | 28.32 | 28.27 | 28.19 | 45.85 | 28.29 | 45.84 | -0.1250 ∈ $I_1$ | 0.1 | 6 |
| 7 | 45.90 | 45.83 | 45.69 | | | | 28.24 | 28.32 | 28.31 | | | | 45.81 | 28.29 | 45.81 | -0.5835 ∈ $I_2$ | 2.8 | 8.8 |
| 8 | 45.78 | 45.72 | 45.75 | 45.89 | 45.66 | 45.84 | 28.36 | 28.41 | 28.23 | 28.36 | 28.34 | 28.31 | 45.77 | 28.34 | 45.83 | -0.3347 ∈ $I_1$ | 0.1 | 8.9 |
| 9 | 45.74 | 45.59 | 46.10 | | | | 28.33 | 28.25 | 28.39 | | | | 45.81 | 28.32 | 45.85 | 0.0508 ∈ $I_1$ | 2.8 | 11.7 |
| 10 | 45.87 | 45.57 | 45.87 | | | | 28.31 | 28.35 | 28.32 | | | | 45.77 | 28.33 | 45.82 | -0.4289 ∈ $I_1$ | 2.8 | 14.5 |
| 11 | 45.70 | 45.75 | 45.78 | | | | 28.31 | 28.28 | 28.31 | | | | 45.74 | 28.30 | 45.76 | -1.2594 ∈ $I_2$ | 2.8 | 17.3 |
| 12 | 45.89 | 45.90 | 45.52 | 45.83 | 46.15 | 45.73 | 28.36 | 28.32 | 28.34 | 28.31 | 28.25 | 28.30 | 45.84 | 28.31 | 45.87 | 0.3295 ∈ $I_1$ | 0.1 | 17.4 |

| | | | | | | | | | | | | | | | | | | |
|---|---|---|---|---|---|---|---|---|---|---|---|---|---|---|---|---|---|---|
| 13 | 45.76 | 46.04 | 45.96 | | | | 28.45 | 28.27 | 28.23 | | | | 45.92 | 28.32 | 45.96 | $1.4140 \in I_2$ | 2.8 | 20.2 |
| 14 | 45.90 | 45.60 | 45.88 | 45.87 | 45.87 | 45.79 | 28.35 | 28.37 | 28.36 | 28.35 | 28.44 | 28.42 | 45.82 | 28.38 | 45.94 | $1.6890 \in I_2$ | 0.1 | 20.3 |
| 15 | 45.82 | 45.79 | 45.92 | 45.88 | 46.07 | 45.84 | 28.32 | 28.31 | 28.32 | 28.30 | 28.32 | 28.33 | 45.89 | 28.32 | 45.92 | $1.3650 \in I_2$ | 0.1 | 20.4 |
| **16** | 45.82 | 46.02 | 45.83 | 45.94 | 45.97 | 45.76 | 28.40 | 28.27 | 28.33 | 28.41 | 28.44 | 28.41 | 45.89 | 28.38 | 46.00 | $\mathbf{2.9287} \in I_3$ | 0.1 | 20.5 |
| 17 | 45.91 | 46.09 | 45.98 | | | | 28.35 | 28.29 | 28.38 | | | | 45.99 | 28.34 | 46.06 | $2.8140 \in I_2$ | 2.8 | 23.3 |
| 18 | 45.79 | 45.92 | 45.83 | 45.75 | 46.31 | 45.87 | 28.35 | 28.31 | 28.36 | 28.38 | 28.28 | 28.32 | 45.91 | 28.33 | 45.97 | $2.2578 \in I_2$ | 0.1 | 23.4 |
| 19 | 45.78 | 45.79 | 45.87 | 45.75 | 45.92 | 46.05 | 28.40 | 28.36 | 28.31 | 28.38 | 28.34 | 28.34 | 45.86 | 28.36 | 45.95 | $1.8157 \in I_2$ | 0.1 | 23.5 |

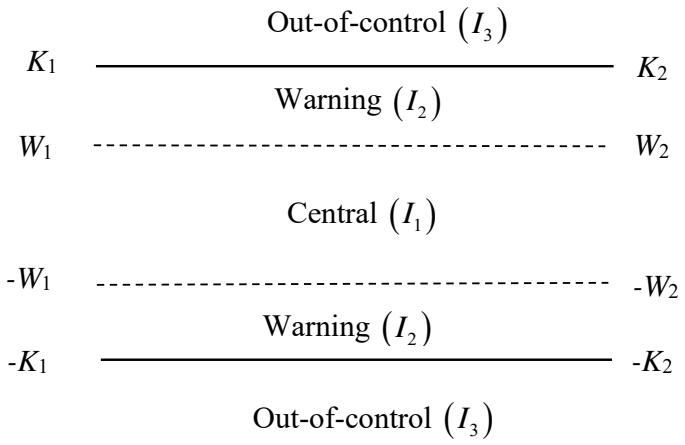


Figure 1. Schematic representation of the VP-AI chart

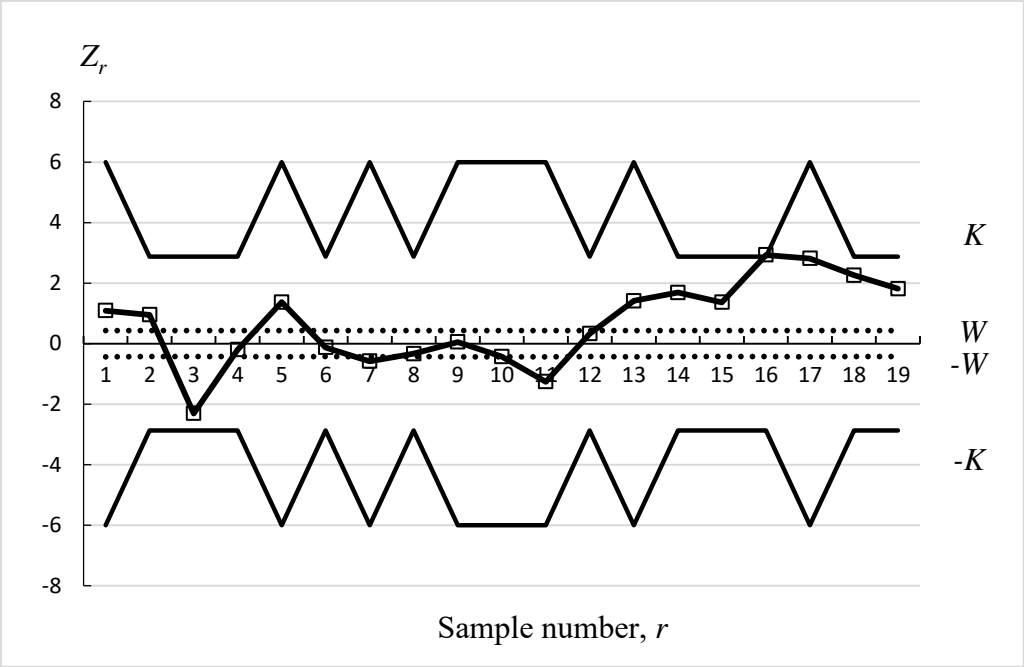


Figure 2. Implementation of the VP-AI chart on the spring manufacturing process